NEODYMIUM AND OXYGEN ISOTOPIC CONSTRAINTS ON UPPER ORDOVICIAN PALEOCEANOGRAPHIC EVOLUTION ACROSS THE DUBUQUE/MAQUOKETA CONTACT IN NE IOWA AND SE MINNESOTA

A Thesis presented to the Faculty of the Graduate School at the University of Missouri-Columbia

---

In Partial Fulfillment of the Requirements for the Degree

Master of Science

---

by

KELSEY ERIN PUTMAN

Dr. Kenneth G. MacLeod, Thesis Supervisor

MAY 2011

The undersigned, appointed by the dean of the Graduate School, have examine the thesis entitled

NEODYMIUM AND OXYGEN ISOTOPIC CONSTRAINTS ON UPPER ORDOVICIAN PALEOCEANOGRAPHIC EVOLUTION ACROSS THE DUBUQUE/MAQUOKETA CONTACT IN NE IOWA AND SE MINNESOTA

Presented by Kelsey Erin Putman,

A candidate for the degree of master of science,

and hereby certify that, in their opinion, it is worth of acceptance.

_____

Professor Kenneth G. MacLeod

_____

Professor Raymond Ethington

_____

Professor Jack Jones

_____

Professor Norlene Emerson

To Mom.

ACKNOWLEDGEMENTS

I would like to thank the National Science Foundation for funding this research through Grant EAR 0545799, as well as financial support from the University of Missouri Department of Geological Sciences, both of which have made this project possible.

I especially would like to thank my thesis advisor, Ken MacLeod, for accepting me as a graduate student and for seeing the potential in my project even before we started. His knowledge and patience in the lab, classroom, and field have been instrumental to this work. Thank you to my committee members, Ray Ethington and Jack Jones for their help and suggestions along the way.

I would also like to thank Norlene Emerson for her support and feedback on this project, as well as Brian Witzke for field assistance and samples.

Thank you to Ellen Martin, Derrick Newkirk, Scott Lepley, and Cheryl Kelley for helping to run samples.

And finally, thanks to all my supportive loved ones.

TABLE OF CONTENTS

List of Figures

List of Equations

List of Photos

Neodymium and oxygen isotopic constraints on Upper Ordovician paleoceanographic evolution across the Dubuque/Maquoketa contact in NE Iowa and SE Minnesota

Kelsey E. Putman

Dr. Ken MacLeod, Thesis Supervisor

ABSTRACT

Measurements of conodonts, phosphatic brachiopods, and authigenic phosphate show no consistent trends in $\delta^{18}O_{phos}$ values but do show a gradual 2-3 unit ε_{Nd} increase across the Dubuque/Maquoketa contact in NE Iowa and SE Minnesota. The lithologic transition between the limestone-rich Dubuque Formation, and the shalely Maquoketa Formation is often marked by a phosphatic hardground. Interpretations from previous studies have suggested that the phosphate was deposited during a time of upwelling of cool, nutrient rich, and oxygen poor water; the longer term shift from Dubuque Formation to the Maquoketa Formation is interpreted as the lithologic expression of a transgressive-regressive subsequence. The relative importance of climatic and circulation changes across the contact was tested along a north-south transect at three locations in IA and MN. Temperature trends were estimated using $\delta^{18}O_{phos}$, and the potential source region(s) of local waters were estimated using ε_{Nd}.

Conodont $\delta^{18}O_{phos}$ paleothermometry was done with conodont separates from samples with high enough conodont abundances ($\leq$250 μm/sample) to yield sufficient Ag_3PO_4 for mass spectrometry analysis. To minimize potential artifacts from inter-species variability, species-specific separates were run for all conodont samples when possible. In addition, mixed separates, inarticulate brachiopods and authigenic phosphate were analyzed in selected samples to increase the number of temperature estimates and to assess the direction and possible magnitude of diagenetic overprinting. To determine if circulation fluctuated over the formational contact, ε_{Nd} values from the phosphatic inarticulate brachiopod, *Leptobolus* were measured. A shift in $\varepsilon_{Nd(t)}$ values would indicate changes in the source regions or in the mixing patterns of water mass(es) in the region.

The $\delta^{18}O_{phos}$ results do not support past models that have invoked upwelling of cool nutrient rich water and/or a transgressive event flooding the carbonate ramp with cool open ocean water as partially responsible for the change in lithologies seen in the Dubuque and Maquoketa Formations, but there is a consistent offset of ~1‰ between the conodonts *Drepanoistodus suberectus* and *Panderodus gracilis*. In addition, ε_{Nd} values from the Dubuque Fm. range from -8.6 to -6.5 and they increase to -5.8 to -4.8 in the overlying Maquoketa Fm. Our results are consistent with a paleoceanographic model influenced by sea level rise. The Dubuque and Maquoketa Formations represent a transgressive-regressive sub cycle with highstand occurring at the contact between the two

formations. During the transgression, fresh-water runoff from the Taconic highlands and an easterly wind could have generated a quasi-estuarine gyre that resulted in surface currents flowing basinward and out of the epeiric sea while cool ocean water flowed into the epeiric sea through the Sebree Trough. The incursion of ocean water and/or runoff from the Taconic highlands is documented by increasing ε_{Nd}. This interpretation and the apparent lack of temperature change suggest that the Dubuque/Maquoketa transition is best interpreted as being forced by circulation patterns, rather than cooling from a climatic event.

CHAPTER 1. Dubuque and Maquoketa Formation Background

1.1. Introduction

As climate change, specifically the switch from one climate regime to the next, becomes a more pressing concern and frequently discussed issue in the scientific community due to the increasing temperature at the earth's surface, the need to look back in earth's history to understand past shifts between greenhouse and icehouse conditions become pertinent. The Late Ordovician is a period of time in earth's history when the climate shifted from a greenhouse state to an icehouse, and back again all within 10's of millions of years (Brenchley et al., 1994; Kump et al., 1995; Saltzman and Young, 2005; Trotter et al., 2008). Atmospheric CO_2 levels in the Ordovician have been estimated to be 8-20 times higher than today (Berner, 1994; Berner and Kothavala, 2001; Herrmann et al., 2003, 2004), yet geologic and isotopic data indicate cooling and glaciation in the Late Ordovician that resulted in the short glacial episode and subsequent mass extinction in the Hirnantian stage (Berry and Boucot, 1973; Sheehan, 1973, 2001; Sepkoski, 1996; Servais et al., 2009). Conodont $\delta^{18}O$ data gathered from epeiric sea samples as well as $\delta^{13}C$ data (where an excursion of $\delta^{13}C$ in the rock record indicates burial of organic matter, and the drawdown of CO_2 in the atmosphere) have been interpreted to indicate cooling through the Late Ordovician, but

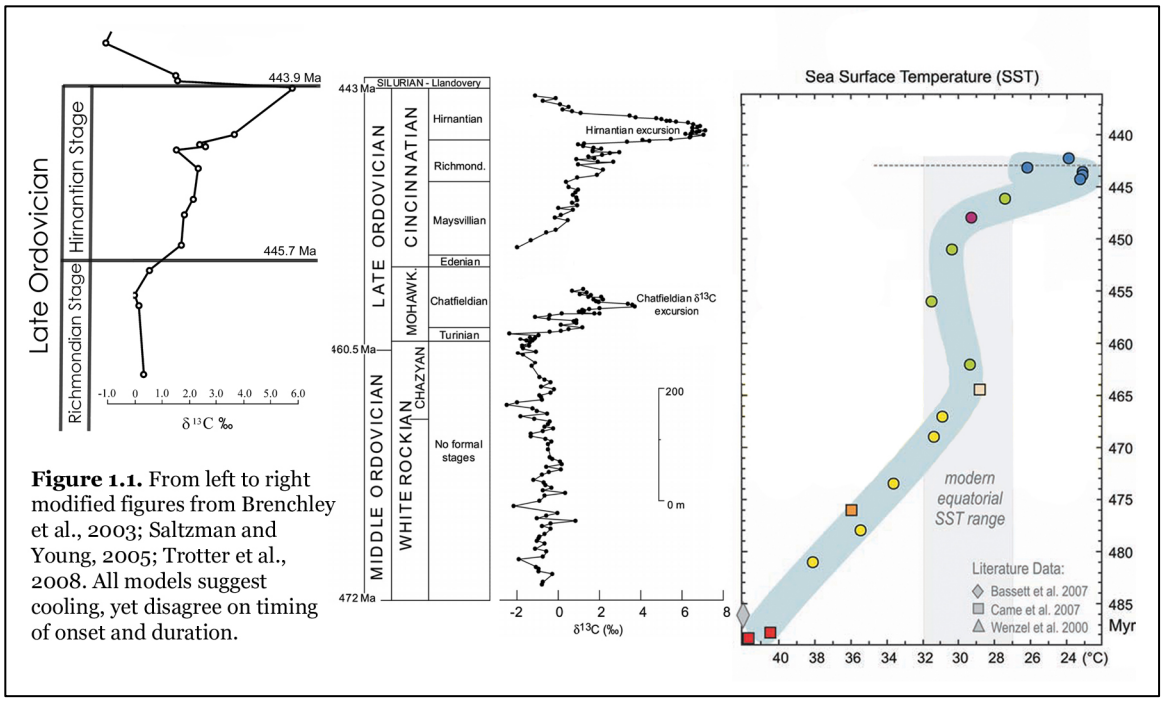

Figure 1.1. From left to right modified figures from Brenchley et al., 2003; Saltzman and Young, 2005; Trotter et al., 2008. All models suggest cooling, yet disagree on timing of onset and duration.

estimates on the timing of cooling range from gradual over ~15 million years (Patzkowsky et al., 1997; Hamoumi, 1999; Pope and Steffen, 2003; Saltzman and Young, 2005, Trotter et al., 2008) to rapid at one million years (Brenchley et al., 2003). Figure 1.1. illustrates 1) a model suggesting a rapid glaciation, constrained by the duration of an $\delta^{13}C$ excursion (Brenchley et al., 2003); 2) a model suggesting two glacial events, interpreted using $\delta^{13}C$ (Saltzman and Young, 2005); and 3) a model of gradual cooling through the Ordovician, with an excursion at the end Ordovician, estimated using $\delta^{18}O$ (Trotter, et al., 2008). Though these three studies are not at the same scale, or use the same isotopes systems, they do all suggest that cooling did occur in the Ordovician.

This study investigates in detail one lithologic transition within the mid-continent Late Ordovician succession that has been interpreted both as the expression of a climatic and a circulation change. The boundary between the

Dubuque and Maquoketa Formations (Upper Mississippi Valley of the Late Ordovician) is marked by the shift from the deposition of limestones in the Dubuque Fm. to shales in the Maquoketa Fm. (Photo 1.1.). The contact between the two Formations often coincides with a phosphate horizon in the lowest Maquoketa Formation which has been interpreted to be the result of an incursion

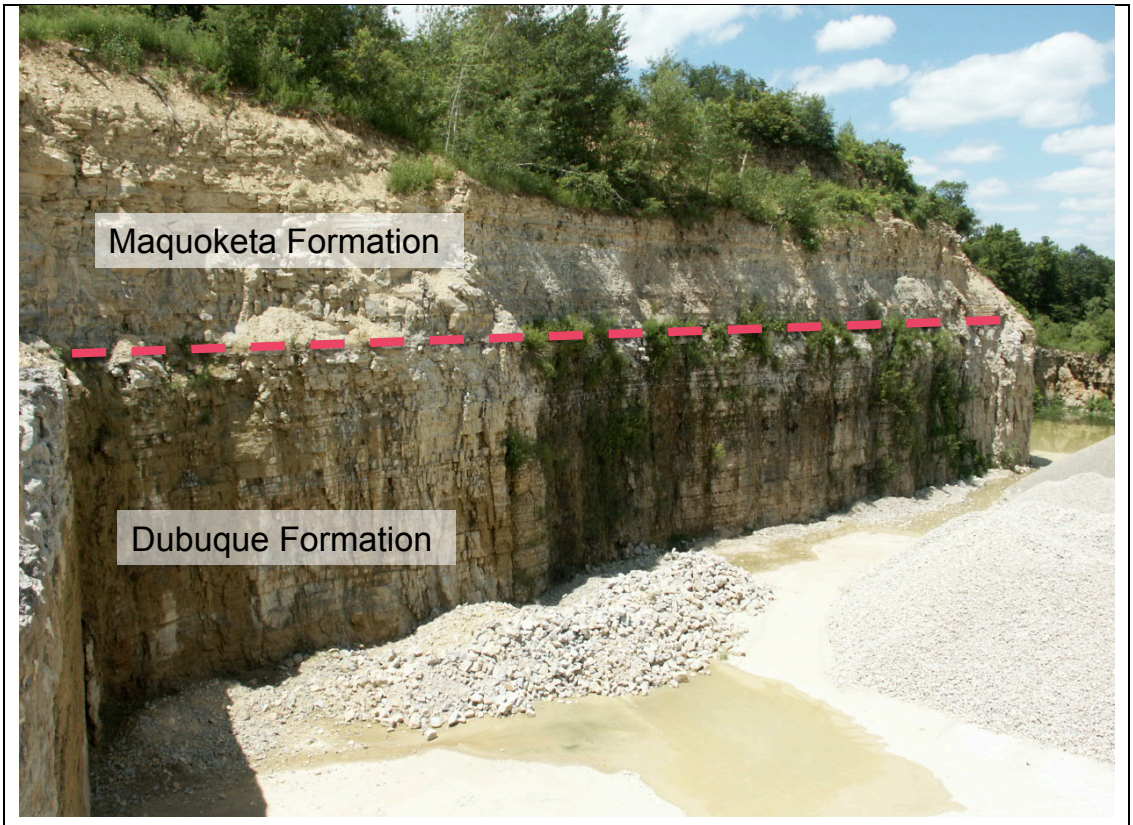

Photo 1.1. An example from the Postville Quarry, IA of the lithologic transition between the Dubuque and Maquoketa Formations. Separating the two formations in a phosphate horizon which is highlighted with a dashed line. Photo by Norlene Emerson.

of cooler, phosphate rich water (Raatz and Ludvigson, 1996; Kolata et al., 2001). Due to the proximity in time to the end Ordovician glaciation and what some workers consider to be precursory cooling events (Raatz and Ludvigson, 1996; Saltzman and Young, 2005) the Maquoketa could represent a time of cooling in the Mid-continent. This project sought to determine the relative importance of

paleoclimatic and/or paleoceanographic factors that led to such transitions over tens of meters of section along a transect ~300 km long; and thereby inform and constrain interpretations of the trends through the Late Ordovician.

Biogenic apatite from conodont elements is increasingly being used to yield $\delta^{18}O$ values to reconstruct paleoclimates of the Paleozoic (Wenzel et al., 2000; Joachimski and Buggisch, 2002; Bassett et al., 2007; Trotter et al., 2008; Herrmann et al., 2010). Carbonates, which were traditionally used in the past for $\delta^{18}O$ studies tend to have low ^{18}O values from recrystallization of the calcite during diagenesis, resulting in unreasonably high estimated sea water temperatures in the Ordovician (Joachimski and Buggisch, 2002; Trotter et al., 2008; Brand et al., 2009;). To reduce the likelihood of diagenetic artifacts, we have used $\delta^{18}O$ values from conodont bioapatite. The phosphate-oxygen bond in the bioapatite is more resistant to diagenetic alteration than that of biogenic carbonates (Wenzel et al., 2000; Vennemann et al., 2002; Trotter et al., 2008). A portion of our study will focus on gathering species-specific separates instead of bulk conodont analysis, which allows us to infer conodont habitat preferences and get a sense of the paleotemperature of the water column at different depths.

The $\varepsilon_{Nd(t)}$ values of phosphatic inarticulate brachiopods were used to estimate water mass circulation across the lithologic contact of the Dubuque Formation and the Maquoketa Formation. Sea-water derived $\varepsilon_{Nd(t)}$ has been used (most notably with respect to this project is the study by Holmden et al. (1998)) to track ocean water circulation changes through time (Holmden et al., 1998). Neodymium isotopic ratios are variable among different oceans and can indicate

source water that was imprinted with the $\varepsilon_{Nd(t)}$ values of rocks of different ages. Nd also has a residence time that is close to or shorter than the mixing time of the ocean (Piepgras and Wasserburg, 1983; Keto and Jacobsen, 1988; Holmden et al., 1998). Establishing neodymium values will enable us to determine if there was a fluctuation in water mass source across the lithologic transition

Conodont $\delta^{18}O$ values were measured on samples from three locations along a south-north transect across northeastern Iowa and southeastern Minnesota. The $\varepsilon_{Nd(t)}$ data were gathered across the lithologic transition at one location. By coupling geochemical analysis of the Dubuque and Maquoketa Formations with established interpretations of the paleoclimatology of the epeiric sea, a more complete understanding of the paleoclimatology at the time of the deposition of the Dubuque-Maquoketa succession can be gained.

1.2. Paleogeography

At the time of deposition of the Dubuque and Maquoketa Formations, North America was rotated clockwise ~90° from its present position and straddled the equator (Pope and Steffen, 2003; Scotese, 1997). What was to become eastern Iowa and Minnesota was under an epicontinental sea and located in a trade-wind belt at ~20° south latitude (Raatz and Ludvigson, 1996; Scotese and McKerrow, 1990; Witzke, 1980). The epicontinental sea, termed the Mohawkian Sea during this time slice, covered the Upper Mississippi Valley of Laurentia and was bounded by the Transcontinental Arch to the paleo-north, the

Wisconsin Arch to the paleo-east, the Ozark Uplift to the paleo-southwest, and the Taconic Highlands to the paleo-southeast (Pope and Steffen, 2003; Raatz and Ludvigson, 1996);

(Fig. 1.2.).

The Transcontinental Arch, located to the north of the trade-wind belt, was positioned well within a humid equatorial zone. During periods of sub-aerial exposure, the arch shed terrigenous clastic sediment into the Mohawkian Sea and served as the source for the clastic sediment of the mixed carbonate- clastic Dubuque Formation (Witzke, 1980; Raatz and Ludvigson, 1996). Similarly, weathering of the Taconic Highlands created a wedge of clastic material that extended from the eastern United States to eastern Iowa, and is likely responsible for the thin shale beds seen in the basal Maquoketa Formation (Raatz and Ludvigson, 1996; Witzke and Kolata, 1988; Witzke, 1980). Current flow from the open ocean and the Taconic Highlands circulated northward,

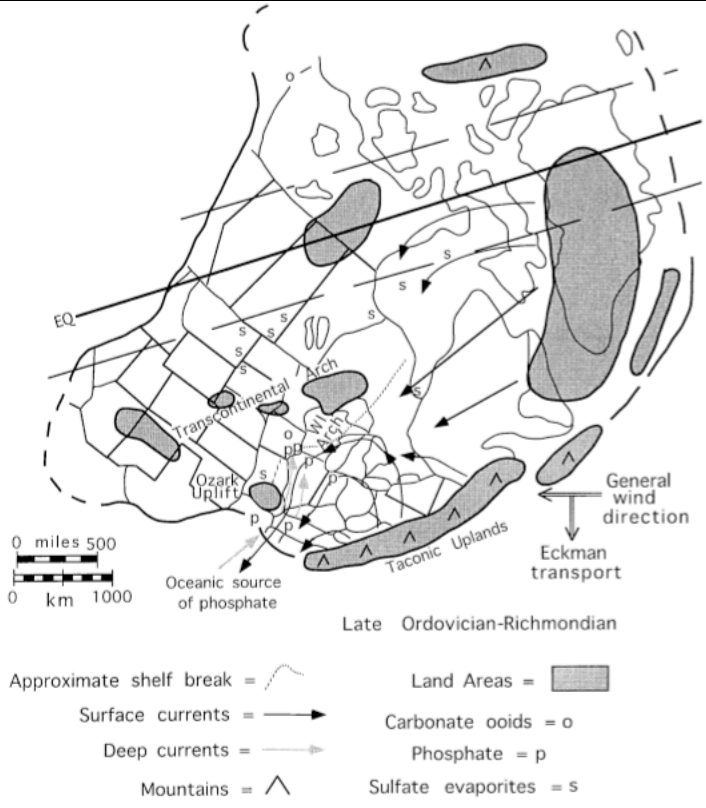

Figure 1.2. Paleogeography of Laurentia during the Late Ordovician (Raatz and Ludvigson, 1996).

entraining clastic material which resulted in the thin shale beds of the basal Maquoketa Formation (Witzke, 1980).

Not all deposits in the Mohawkian sea were dominated by clastic deposition; overall, the midcontinent depositional system of Laurentia during the Late Ordovician has been characterized as a shallow sub-tidal carbonate ramp (Pope and Steffen, 2003) with no shelf slope break and low rates of sedimentation (Kolata et al., 2001). These carbonate ramp deposits are largely present in the Dubuque Formation, but minor carbonate beds are interspersed within the shales of the Maquoketa Formation. Relative paleobathymetry has been estimated based on lateral facies geometries and assumed to be 10's-100's of meters deep. Raatz and Ludvigson (1996) provided a unique method for estimating the depth of the Mohawkian Sea in eastern Iowa during deposition of the lowermost Maquoketa Fm. by measuring nautiloid septal implosion. The abundant nautiloid, *Isorthoceras sociale* at Graf, Iowa can be found with the weaker anterior septa imploded, a result of the ambient water pressure overcoming the strength of the septa (Raatz and Ludvigson, 1996). Based on the following equation:

Depth of implosion= [100(131 MPa/ {septal radius/ 2 septal thickness})]- 10 m Eq 1.1.

depth at the time of implosion can be estimated. Through this calculation

Raatz and Ludvigson (1996) report an average depth of implosion to have been ~200 m, thus estimating a depth of ~200 m for this portion of the epeiric sea in the middle of the sample transect for this project.

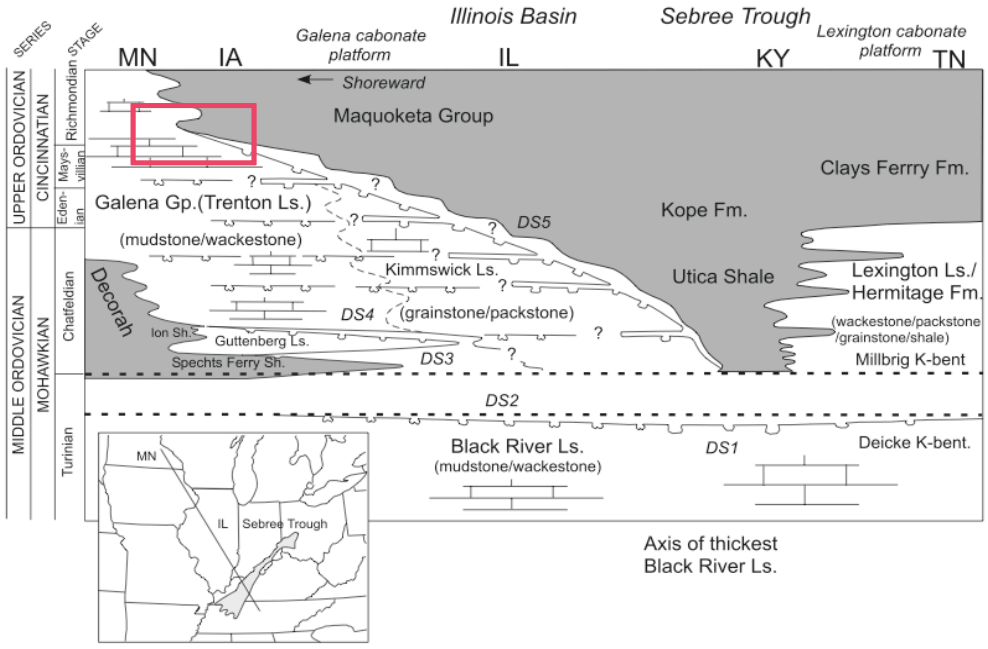

Figure 1.3. Illustration of the sub-tidal carbonate ramp, with the shale filled Sebree Trough highlighted in cross section as well as map view. Research localities have been highlighted in a pink box for reference (Fanton and Holmden, 2007; modified after Kolata et al., 2001).

This carbonate ramp was not laterally continuous from the western margin of the sea to the Taconic Highlands. Subsurface data from western Kentucky, southern Indiana, and western Ohio indicates a linear shale-filled structure that is estimated to be ~400 km long and ~150 km wide in western Tennessee, then tapers to 25 km wide or less in southern Indiana (Kolata et al., 2001). This structure (Fig. 1.3.) has been interpreted as a paleobathymetric low, and has been named the Sebree Trough (also identified as the Sebree Valley, or Kope Trough),

(Kolata et al., 2001). Further investigation of the trough geometry suggests that the trough extended south into east-central Arkansas into what was the southern continental margin of Laurentia (Kolata et al., 2001; Witzke, 1980). Through the use of K-bentonite stratigraphy (which uses phenocrysts and chemical fingerprinting to identify bentonite layers that are laterally continuous from the Taconic Highlands to Iowa) and biostratigraphy for age control, it is believed that the Sebree Trough began to develop during the late Turinian to early Chatfieldian stages of the Mohawkian Series (Kolata et al., 2001). The stratigraphy places the initiation of trough development in the Middle Ordovician, well before deposition of the Dubuque Formation and Elgin Member, which was deposited in the early Richmondian stage (Fig. 1.4.) in the Cincinnatian Series (Kolata et al., 2001).

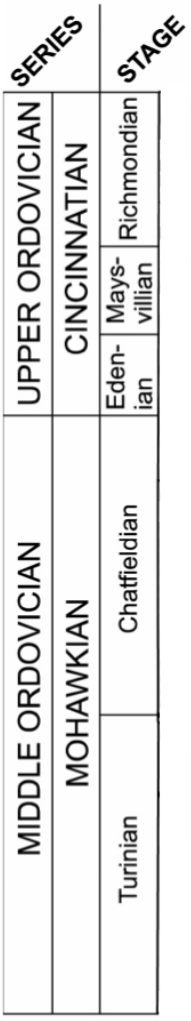

Figure 1.4. Chronostratigraphy places the Dubuque Fm. at the end of the Maysvillian Stage and the Maquoketa Fm. at the beginning of the Richmondian Stage. Sebree Trough development has been estimated to have begun in the late Turinian to early Chatfieldian (modified after Kolata et al., 2001).

The trough was situated on top of the failed Late Precambrian-Early Cambrian Reelfoot Rift and it is possible that the increased subsidence that produced the trough in the late Turinian is the result of far-field tectonic effects from the Ordovician Taconic orogeny (Kolata et al., 2001). Characterized by deep-water facies (Fanton and Holmden, 2007) the Sebree Trough also features hardground omission surfaces and localized phosphogenesis (Kolata et al., 2001).

The Sebree Trough was not only a large paleogeographic feature, it also played an important role in the paleoceanography of the region. Because the Sebree Trough extended to the southern margin of the epeiric sea and was connected to the Iapetus Ocean, it was able to act as an avenue for open ocean water incursion into the epeiric sea. (Kolata et al., 2001) A more detailed discussion of the Sebree Trough and its influence on the regional paleoceanography is explored in the following section.

1.3. Paleoceanography

The many models of the paleoceanography of the Upper Ordovician Mohawkian sea have been broken down into the most vital components and are described in detail in the following subsections: 1.3.1. Estuarine circulation, 1.3.2. Upwelling and Stratified Water Column, and 1.3.3. Transgressive-Regressive Subsequence.

During the Middle and Late Ordovician, the North American craton experienced one of the largest marine transgressions of the Phanerozoic (Witzke, 1980; Simo et al., 2003). This flooding of the craton created a vast interior ocean (the Mohawkian Sea) for which there is no modern analogue (Witzke, 1987; Allison and Wells, 2006). A water balance equation for an epicontinental sea can be developed with the following parameters:

1) freshwater influx via rainfall and river/aquifer discharge

2) evaporation

3) in-flow of water from the open ocean, and

4) outflow to the ocean

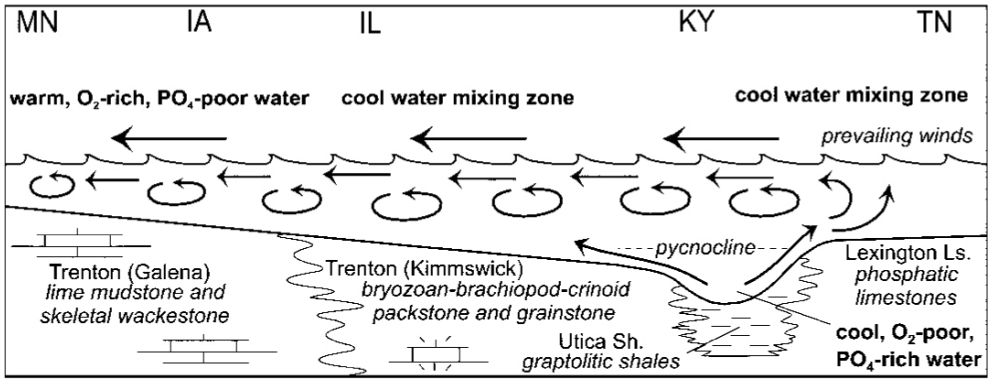

Figure 1.5. A generalized atmospheric and oceanic circulation model of a north-west to south-east transect illustrating the associated lithologies (Kolata et al., 2001)

This relationship between evaporation, the influx of freshwater and wind, can lead to large-scale circulation patterns (Witzke, 1987). Based on these parameters, wind circulation, and paleogeography, a model including quasi-estuarine circulation (QEC), upwelling, and a stratified water column has been proposed for the epeiric sea during the deposition of the Dubuque and Maquoketa Formations (Witzke, 1987; Raatz and Ludvigson, 1996; Ludvigson and Witzke, 2004). In this model, a quasi-estuarine current, which is similar to the smaller scale "estuarine" circulation found in estuaries where the freshwater input exceeds evaporation, was driven by easterly surface winds and fresh-water runoff from the Taconic Highlands, as opposed to normal estuarine circulation where density differences controls most flow (Witzke, 1987; Raatz and Ludvigson, 1996). Much of the surface flow was parallel to the Transcontinental Arch, while Eckman flow transported the remainder of the surface flow basinward (Raatz and Ludvigson, 1996). A lens of relatively fresh water, sourced

from topographic highs such as the Taconic Highlands, could have developed above the more saline bottom water, where surface winds would have driven a quasi-estuarine dominated current (Witzke, 1987). Open ocean water flowed into the Mohawkian Sea through the Sebree Trough to replace the out flowing surface waters (Fig.1.5.).

1.3.1. Quasi-estuarine circulation

It has been suggested that the primary mode of seawater circulation in the Mohawkian sea was a quasi-estuarine circulation (QEC) system (Witzke, 1980, 1987; Raatz and Ludvigson, 1996; Kolata et al., 2001; Ludvigson et al., 2004; Fanton and Holmden, 2007). Such a circulation pattern can be established when the rate of fresh water influx exceeds that of evaporation (Witzke, 1987). It is believed that a quasi-estuarine circulation pattern differs from estuarine circulation in that the main driving force of circulation is not just thermohaline processes, but also influenced by wind (Witzke, 1987). Applying this principle to the Mohawkian sea during deposition of the Dubuque and Maquoketa Formations, fresh water runoff from the Taconic Highlands as well as other topographic highs would have been greater than the overall net evaporation in the basin, creating a lens of fresh water on top of saline bottom water (Witzke, 1987).

As mentioned in the previous section, the paleogeographic position of the epicontinental sea at 20° S would have placed the epeiric sea in a belt of easterly

winds. Combining these easterly winds with Coriolis deflection (Kolata, 2001) then promoted westerly transport of the surface waters out of the basin at the Ouachita continental margin (Witzke, 1987). These westerly flowing currents are believed to be the transport mechanism for the clastic material of the Maquoketa Formation (Witzke, 1987). In this model an influx of freshwater that entrained siliciclastics in the suspended load from the Taconic highlands (clastic debris from the Martinsburg, Juniata, and Sequatchie Formations) prograded westward to create a clastic wedge (Witzke, 1987; Raatz and Ludvigson, 1996; Kolata et al., 2001) that is responsible for the shale deposits of the Elgin Member, the lowest member of the Maquoketa Formation.

1.3.2. Upwelling and Stratified Water Column

The upwelling of nutrient rich, cool water has been invoked as an integral portion of the paleoceanography of this region during the Late Ordovician (Witzke, 1987). It has been suggested by Raatz and Ludvigson (1996) that the net surface transport of water out of the epeiric sea basin resulted in the drawing up of phosphate rich, anoxic deep water to the surface, forming an area of upwelling.

Upwelling can occur in seas where surface flow diverges, typically induced by wind, and vertical flow from depths (<300 m) brings nutrients to the surface waters (Witzke, 1987). In modern examples, the upwelling water mass comes from depths that do not surpass a few hundred meters (Witzke, 1987). A stratified water column is also cited as a characteristic component of the

Mohawkian Sea (Holmden et al., 1998, Panchuk et al., 2006, Kolata, 2001, Raatz and Ludvigson, 1996). A pycnocline developed when a denser dysaerobic to anaerobic bottom water mass was below a warm, oxygenated water mass (Witzke, 1980, 1987; Raatz and Ludvigson, 1996; Kolata, 2001). Though stratification does not always lead to anoxia, the geologic evidence for this dysaerobic to anaerobic bottom water is evident in the laminated black and brown organic rich shales present in the Maquoketa Formation as well as the lithologies above and below the Maquoketa and Dubuque Formations (Witzke, 1987), suggesting that at least episodically, the rate of aerobic decay was sufficient to use more oxygen than was being added to the bottom waters (Allison and Wells, 2006).

1.3.3. Transgressive- Regressive Subsequence

In addition to the above circulation models, evidence exists for a transgressive-regressive subsequence spanning the deposition of the Dubuque and Maquoketa Formations that has been applied in many models (Kolata et al., 2001; Witzke, 2005; Fanton and Holmden, 2007; Leslie, 2009)(Fig. 1.6.). Witzke and Bunker (1996) and Raatz and Ludvigson (1996) interpreted the Dubuque Formation to have been deposited during a transgression. The hardground and associated phosphate interval is believed to represent a period of sediment starvation, with the dark brown organic rich shale marking the point of highstand (Fig. 1.7.) (Witzke and Bunker, 1996; Raatz and Ludvigson, 1996; Fanton et al., 2007). Through the remainder of the measured section of this study clastic

deposits are common and likely were derived from Taconic clastic sources (Witzke, 1980, 1987; Raatz and Ludvigson, 1996).

Some of these models have suggested that open ocean water flowed into

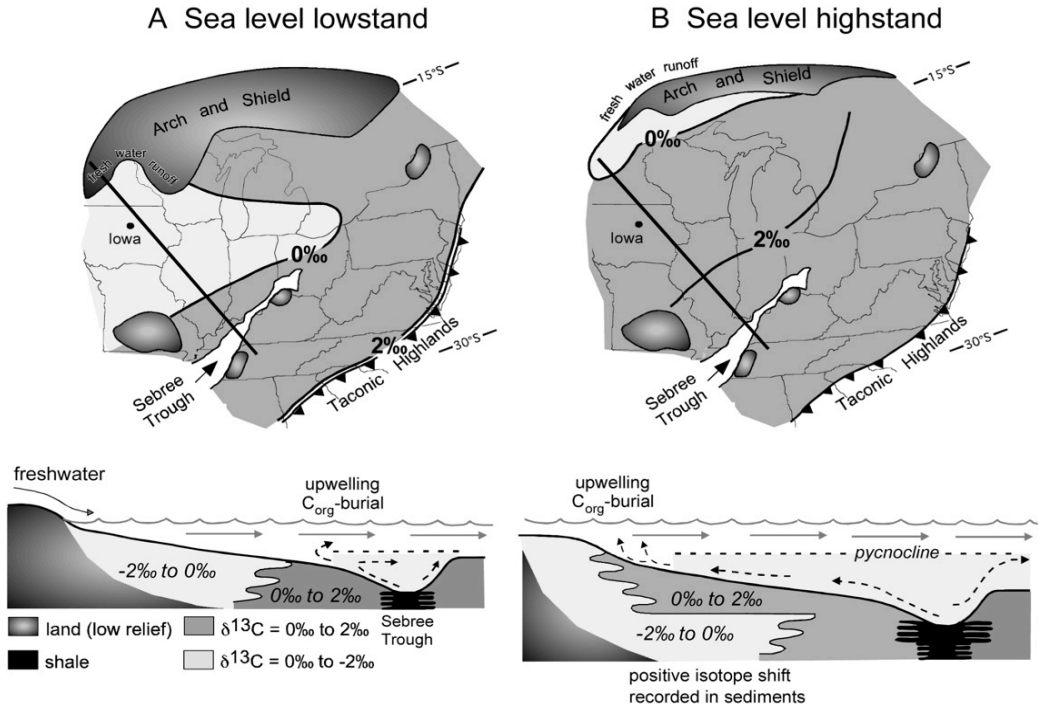

Figure 1.6. Sea level forcing of the regional C cycle, interpreted from a transgressive-regressive viewpoint. (A) At low sea level there is restricted flow between the proximal and distal portions of the sea, and the pycnocline is more localized around the Sebree Trough. QEC flow is also supported by freshwater run off from topographic highs. (B) At high sea level the QEC flow strengthens, as well as expands the pycnocline. Upwelling of nutrient rich water from the Sebree Trough results in an increase in productivity, reflected in the shift to higher $\delta^{13}C$ values (Modified after Fanton and Holmden, 2007).

the Mohawkian Sea via the Sebree Trough, offering an additional instance for cool water to flood the carbonate ramp (Kolata et al., 2001; Fanton and Holmden, 2007). Through the development of a pycnocline around the Sebree

Trough, cool eutrophic waters were localized below the pycnocline in the Trough (Fanton and Holmden, 2007). During the transgression, an influx of open ocean water resulted in the cool eutrophic waters to flow up the carbonate ramp (Fanton and Holmden, 2007). By this model, cooling should have occurred while the Maquoketa Formation was deposited and be reflected in the $\delta^{18}O$ values.

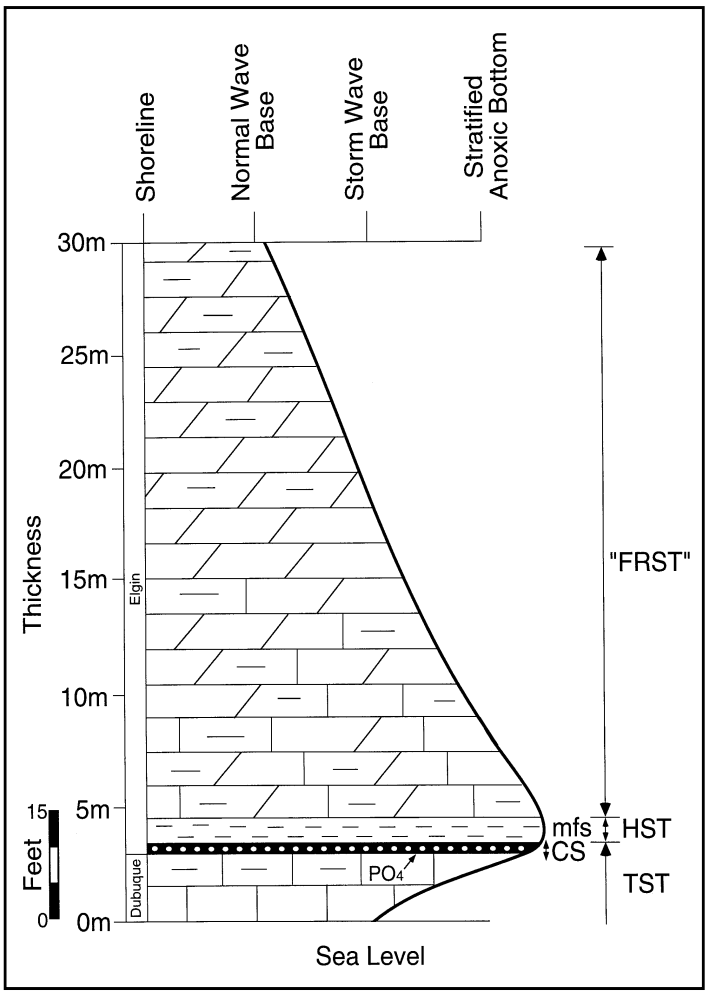

Figure 1.7. Transgressive-regressive subcycle of the Dubuque-Maquoketa Formations (Modified after Raatz and Ludvigson, 1996).

CHAPTER 2. Stable Isotope Methods

2.1. $\delta^{18}O$ Paleothermometry Background

The overarching requirements for developing an isotope based paleothermometer are to devise a method that has minimal unknown (or unconstrained) variables, has little diagenetic overprinting of isotopic signals, and measures a material(s) that is common throughout geologic time. Even though many ingenious methods have been developed and good scientific progress has been made, no one method has been discovered that includes all of these desirable traits. This project utilizes the $\delta^{18}O$ bioapatite paleothermometer to try to determine whether seawater temperatures fluctuated during the deposition of the Dubuque and Maquoketa.

The ratio of the ^{18}O isotopes to the ^{16}O isotopes in biogenic apatite or carbonate are measured to estimate paleotemperature in ocean water. When at equilibrium, the oxygen present in phosphate is enriched with the heavy oxygen isotope, ^{18}O, relative to the water in which the mineral precipitated. The fractionation between the phosphate (or carbonate) and water is a function of temperature where fractionation decreases as temperature increases. Thus, the difference between $\delta^{18}O_{phosphate}$ and $\delta^{18}O_{water}$ can be used to determine the temperature of the water at the time of mineral was precipitation.

This method is adventageous for estimating paleotemperatures because of: 1) the enzyme-catalyzed oxygen isotope exchange between phosphate and water during bioapatite secretion (which lowers the activation energy and increases the rate of the reaction), results in a rapid exchange of oxygen on the order of minutes; 2) on the geologic time scale the isotopic exchange of oxygen between phosphate and water is very slow at low temperatures; 3) phosphate-oxygen bonds are more resistant to alteration through diagenesis than carbonate-oxygen bonds; 4) the oxygen found in the strong bond of PO_4^{3-} may be isolated for isotopic analysis minimizing potential contamination from the oxygen found elsewhere in the bioapatite formula ($Ca_5(PO_4, CO_3, F)_3(OH, F, Cl, CO_3)$); and 5) bioapatite (phosphate) is secreted in isotopic equilibrium with its environmental fluid (in this case, seawater) (Longinelli and Nuti, 1973; Kolodny et al., 1983; Crowson et al., 1991).

Therefore, paleotemperature can be estimated based on the oxygen isotopic composition of bioapatite skeletal material using the following equation by Longinelli and Nuti (1973):

$$t°C = 111.4 - 4.3(\delta^{18}O_p - \delta^{18}O_w) \qquad \text{Eq. (2.1.)}$$

where t is the temperature of the water in °Celsius; $\delta^{18}O_p$ is the $\delta^{18}O$ values from phosphate in the bioapatite grain, and $\delta^{18}O_w$ is the assumed value of $-1‰_{VSMOW}$ to account for an ice-free earth scenario. A major complication in the use of $\delta^{18}O$ conodont paleothermometry is that the equation used to derive a

temperature from oxygen isotopes includes three variables, temperature, $\delta^{18}O_{sample}$ and $\delta^{18}O_{seawater}$. The $\delta^{18}O_{seawater}$ is commonly assumed to be -1 relative to the V-SMOW (Vienna standard mean ocean water) standard to account for an ice-free earth scenario and $\delta^{18}O_{sample}$ is measured in the lab. Temperature is then estimated using Eq. 2.2.

Because seawater values are assumed, errors in this estimate could compromise paleotemperatures estimates. Polar ice sheets concentrate water molecules with ^{16}O, the lightest of the stable oxygen isotopes. This phenomenon is due to the slight tendency for water molecules composed of ^{16}O to evaporate preferentially over water molecules containing the heavier oxygen isotope and for water molecules containing ^{18}O, to preferentially condense out of water vapor. The growth and decay of glaciers is then able to change the isotopic composition of the seawater based on the storage of ^{16}O rich glacial ice, and its subsequent reintroduction into the hydrologic cycle with the melting of glacial ice. On a regional scale, the balance of evaporation vs. precipitation will determine the oxygen isotopic composition of the local waters, and then affect the oxygen isotopic composition of organisms or mineralized tissue that precipitate skeletons in that same ocean water.

Early in the development of this method, it was believed that measuring the oxygen isotope compositions of both the phosphate and calcite in shells (from the same samples) would yield paleotemperatures as well as the isotopic composition of the water that the organism precipitated its shell (Urey et al.,

1951). This aspect of the method proved to be incorrect, as the $\delta^{18}O$ paleotemperature equation for carbonates, modified by Craig (1965):

$$t°C = 16.9 - 4.2(\delta_c - \delta_w) + 0.13(\delta_c - \delta_w)^2 \qquad \text{Eq. (2.2.)}$$

and the equation (Eq. 2.1.) for phosphate used by Longinelli and Nuti (1973) resulted in nearly identical slopes so the isotopic composition of water can not be meaningfully constrained by measuring the $\delta^{18}O$ values of carbonate/phosphate pairs.

Conodonts, mineralized (bioapatite) jaw-like elements from proto-vertebrates, can be used to generate $\delta^{18}O$ values for paleotemperature reconstructions. A detailed description of this method can be found in the Materials and Methods section. Conodonts also prove useful as they have been extensively studied in the past for biostratigraphy and are well understood through much of the Paleozoic. Conodonts with little thermal alteration (Herrmann et al., 2010), which can be estimated using the conodont alteration index based on color, are preferred specimens for $\delta^{18}O$ studies. The light amber color of conodonts that have only gone through minor thermal are thought to be most likely to preserve original $\delta^{18}O$ values. Since conodont can be found in rocks from the late Cambrian to the early Triassic, they are quite useful for paleothermometry studies extending back into the Ordovician.

2.2. $\varepsilon_{Nd(t)}$ Paleocirculation Background

The $^{143}Nd/^{144}Nd$ ratio of ancient seawater can be used to estimate paleocirculation through time and is a powerful tool in paleoceanograhy. Phosphates and biophosphates are the best materials to sample for obtaining paleoceanic neodymium values (Keto and Jacobsen, 1988) because of their high rare earth element (REE) contents (Holmden et al., 1996). Studies show that the bulk of the Nd is acquired very quickly, on the 1000 year timescale, at or just below the sediment- seawater interface and reflect the same REE pattern of contemporaneous bottom seawater (Scher and Martin, 2004; Keto and Jacobsen, 1987; Holmden et al., 1996). In the case of analyzed fish teeth, a post-mortem mineralogical transformation of the teeth takes place from hydroxyfluorapatite to fluorapatite at the sediment-water interface (Martin and Scher, 2004) whereby the teeth acquire Nd isotopic ratios reflective of the bottom water Nd signal (Scher and Martin, 2004).

The budget for Nd in each ocean basin is determined by continental sources (Keto and Jacobsen, 1988). Both modern oceans and paleoceans have large variations in their $^{143}Nd/^{144}Nd$ due to the short residence time of Nd in ocean water (Keto and Jacobsen, 1988). The residence time of Nd is estimated to be between 600-2000 years, which is close to or shorter than the mixing of the ocean making neodymium isotope ratios a suitable parameter to study to infer paleocirculation (Tachikawa et al., 1999).

The ratio of $^{143}Nd/^{144}Nd$ from different water bodies are reported in ε_{Nd} values, which are defined as how much the sample $^{143}Nd/^{144}Nd$ ratio deviates from the bulk Earth $^{143}Nd/^{144}Nd$ (Keto and Jacobsen, 1988). Neodymium values can vary over time in an ocean basin and are related to the release of Nd through weathering of volcanic rocks (Keto and Jacobsen, 1988). The ε_{Nd} value of seawater is directly related to the average age(s) of the continental Nd sources (Keto and Jacobsen, 1988). The ε_{Nd} values range between ~+5 to +10 for young volcanic arc rocks; and range between ~- 20 to -35 in Archean shields. The ε_{Nd} values for average crust range between ~ -15 to -17 (Keto and Jacobsen, 1988). Each basin can have different ε_{Nd} values, and will be an average ε_{Nd} value of the river(s) drainage basin(s).

The ε_{Nd} values of small oceans have the possibility of being controlled by circulation patterns and these circulation changes can be caused by tectonics, climate change, or changes in sea level (Keto and Jacobsen, 1988). To accurately interpret the ε_{Nd} patterns from paleoceans, the paleogeography, circulation changes, erosional effects on the Nd input, and the age of rocks needs to be considered. In relation to this study, we have taken into account the possible water mass(es) that might be identified, and what kind of ε_{Nd} values can be expected based on the water mass provenance. Based on data from Holmden et al., (1998), waters with ε_{Nd} values indicative of the Mid-continent, the open ocean, and the Taconic Highlands were all present in the Mohawkian Sea during the deposition of the Dubuque and Maquoketa Formations.

2.3. Materials and Methods

The $\delta^{18}O$ values from bioapatite grains can be used to estimate ancient water temperatures (Joachimski and Buggisch, 2002, Vennemann et al., 2002, Bassett et al. 2007, Trotter et al., 2008). In order to estimate paleocean temperatures of the Late Ordovician epicontinental sea, $\delta^{18}O$ values of phosphate in conodont elements and other phosphate grains (generalized formula: $[Ca_5(PO_4, CO_3, F)_3(OH,F,C,CO_3)]$ although considerable variability can exist (Vennemann et al., 2001)]) were measured. Water temperatures may be estimated from $\delta^{18}O_{phosphate}$ values of bioapatite grains using Eq. 2.1. described the $\delta^{18}O$ Background section.

2.3.1. Sample Collection

Bulk rock samples were collected at seven locations in eastern Iowa and southeastern Minnesota along a north-south transect (Fig. 1.8). From south to north sample localities were as follows:

- South Williams drill core in Louisa Co., IA (SW ¼, SW SW Sec. 20, T74N, R4W)
- Webber Quarry in Dubuque, Dubuque Co., IA (N 42° 29'04.7", W 090° 44'38.1")
- Postville Quarry and Highway 51 road cut in Allamakee Co., IA (N 43° 07'36.7", W091° 33'59.7")

- Big Springs Core in Clayton Co., IA (SE SE Sec. 10, T94N, R6W)
- Graf Road outcrop, Graf, Dubuque Co., IA (N 42°29'22.4", W 090° 52'29.6)
- Highway 20 outside of Dubuque, in Dubuque Co., IA (N 42° 27'56.2", W 090° 46'05.4")
- Rifle Hill Quarry in Fillmore Co., MN (N 43°36'1", W 92°14'49")

Fieldwork focused on the Ordovician outcrop belt of central Iowa and southern Minnesota because of the abundance of described exposures in this district (e.g. Raatz & Ludvigson, 1996; Witzke et al., 1997). In addition, to the south of the sampled locations, Ordovician rocks are no longer exposed or have been altered by Mississippi Valley Type mineralization (Witzke and Ludvigson, 2005); and to the north of the research transect, the rocks are highly dolomitized (Witzke and Ludvigson, 2005). Locations were selected with help from Brian Witzke of the Iowa Geological Survey and Norlene Emerson of the University of Wisconsin-Richland with the goal of recovering a record that spanned the lithologic transition from the Dubuque to Maquoketa formations, with as wide geographic coverage as possible. Core material was provided by Brian Witzke and Bill Bunker from the Iowa Survey's core repository.

Samples were collected (~1-2 kilograms) at .5- 1.5-meter intervals through each measured section, and sample locations were recorded with a GPS unit. The Big Springs core and Highway 20 and Graf locations were sampled as pilot studies; a few samples from these sites were collected from outcrop float or

isolated portions of the outcrop/core. Samples were then processed in the laboratory at the University of Missouri- Columbia.

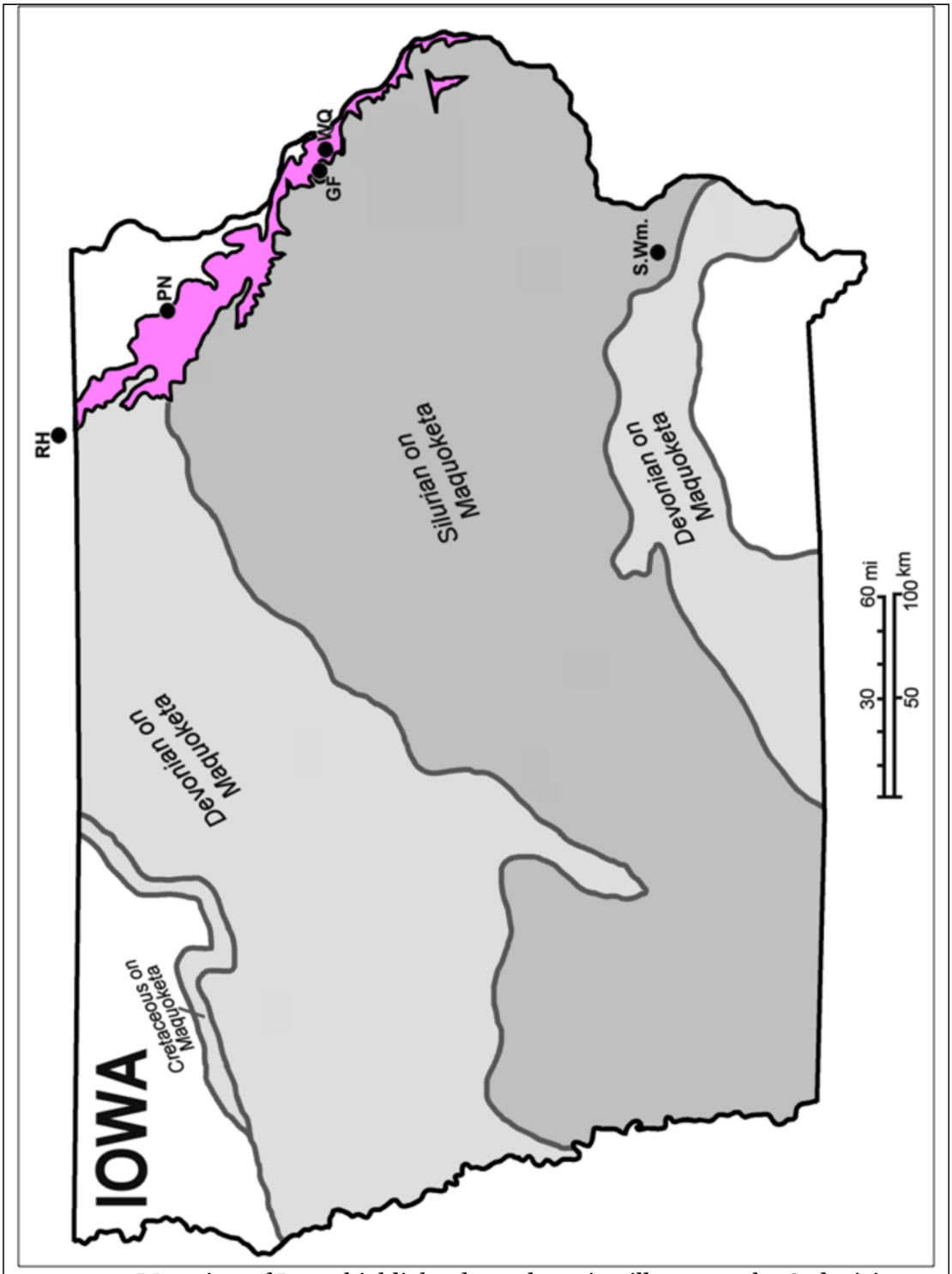

Figure 1.8. Map view of Iowa; highlighted purple region illustrates the Ordovician outcrop belt. Select sample sites illustrated as: S. Wm: South Williams Core, GF: Graf Roadcuts, WG: Webber Quarry, PN: Postville Roadcut and Quarry, and RH: Rifle Hill Roadcut and Quarry, MN (Modified from Witzke).

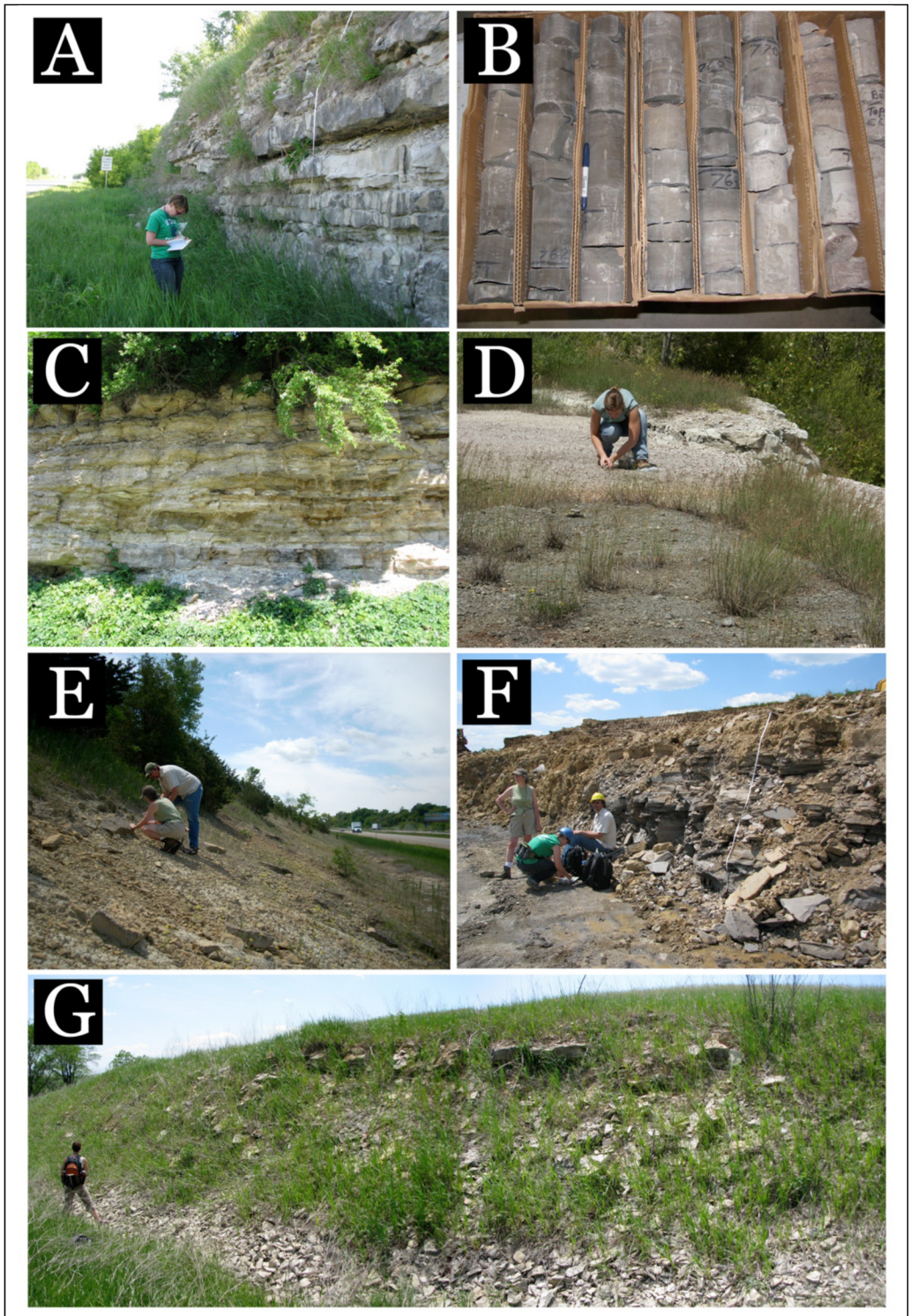

Photo 2.1. Photos of research locations. (A) Dubuque Formation, Postville Roadcut, IA. (B) Dubuque and Maquoketa Formations, South Williams Core, IA. (C) Maquoketa Formation, Graf, IA. (D) Basal phosphorite, Postville Quarry, IA. (E) Dubuque Formation, Highway 20, IA. (F) Basal phosphorite and Maquoketa Formation, Webber Quarry, IA. (G) Maquoketa Formation, Rifle Hill Roadcut, MN. Photos A, B, C, F, G by Ken MacLeod. Photo E by Kelsey Putman. Photo D by Norlene Emerson.

2.3.2. Laboratory Methods

2.3.2.1. *Acid Dissolution*

Bulk rock samples were crushed to ~1.5 cm pieces and then dissolved in approximately 2.5 L of a 15% solution of 1 M Glacial Acetic acid (CH_3COOH) for each kilogram of sample. Samples typically took 2-3 weeks to dissolve. Samples that were more resistant to dissolution (typically Maquoketa shale samples) were dissolved in a calcium phosphate buffered 10% Formic acid (HCO_2H) solution for one week.

Once visible reactions (i.e., bubbling) stopped, the remaining insoluble material was wet rinsed in a set of nested sieves (1 mm, 710 μm, 63 μm). Sediment smaller than 63 μm was discarded, sediment larger than 1 mm was saved for additional acetic acid dissolution, and sediment which remained on the 63 μm and 710 μm sieves was retained for retrieving conodonts. All retained sediment was dried in an oven at 50°C . The dried 63 μm and 710 μm size fractions were then dry sieved (500 μm, 250 μm, 125 μm). Conodonts in these samples rarely were larger than 500 μm or smaller than 125 μm, so sediment samples were high-graded by dry sieving to retain the most conodont-productive size fractions of 250 μm and 125 μm. If the sand sized insoluble residue was less than 30 g, it was picked directly for conodonts and not processed further.

2.3.2.2. *Heavy Liquid Separation*

After acetic acid dissolution, samples that yielded >30 grams of sand sized insoluble sediment residue were further processed using heavy liquid separation in order to concentrate conodonts. The heavy liquid tetrabromoethane, $CHBr_2$ $CHBr_2$, was used and has long been the preferred heavy liquid utilized in density separation of conodonts (Branson and Mehl, 1933; Austin, 1987). Tetrabromoethane (TBE), with a density of 2.94 g cm $^{-3}$, is less dense than the average conodont that has a density between 2.90-3.04 g cm^{-3} (Austin, 1987). This difference in densities makes it possible to concentrate most of the conodonts whereby light material floats to the top of the TBE while conodonts and other dense grains sink to the bottom. To avoid cohesion between grains and "rafting" of conodonts in the rising less dense material, the separatory funnel was periodically swirled to disperse the floating mass of grains so that the conodonts could more easily settle to the bottom of the funnel.

The dense fraction at the bottom of the funnel was collected onto 150 mm filter paper and rinsed with Acetone (CH_3COOH_3). Samples were then dried overnight using a 35° C hot plate in the fume hood in order to drive off residual TBE.

2.3.2.3. *Conodont Picking and Identification*

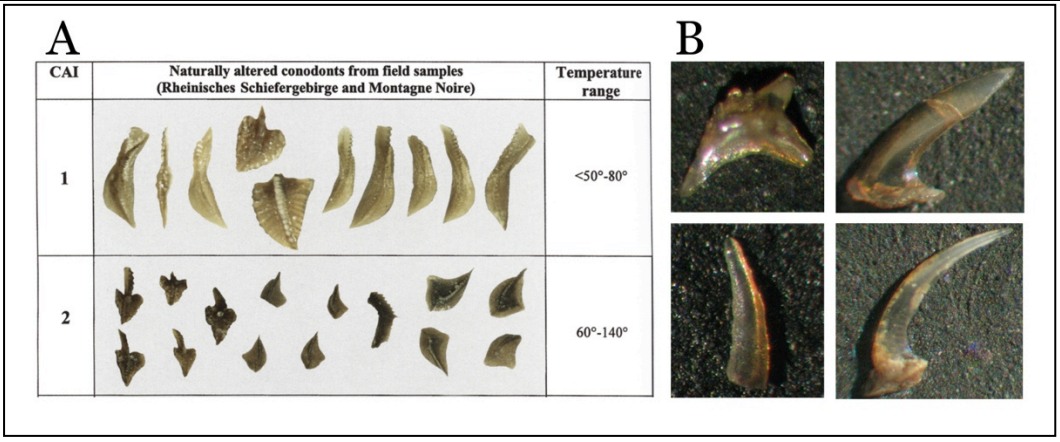

Photo 2.2. (A) The conodont color alteration index (CAI) illustrating conodonts with a CAI from 1-2 (Modified from Konigshof, 2003). (B) Examples of conodonts used in this study with a CAI less than 2 (Photos by Kelsey Putman).

Conodonts and other grains were hand-picked from the heavy liquid sample residue under a binocular microscope using a paintbrush wetted with de-ionized H_2O and then transferred to an assembly slide. Conodont elements were separated by species and identified with assistance from Dr. Ray Ethington. All recovered conodonts are light amber in color, rating less than two on the conodont color alteration index which indicates good preservation

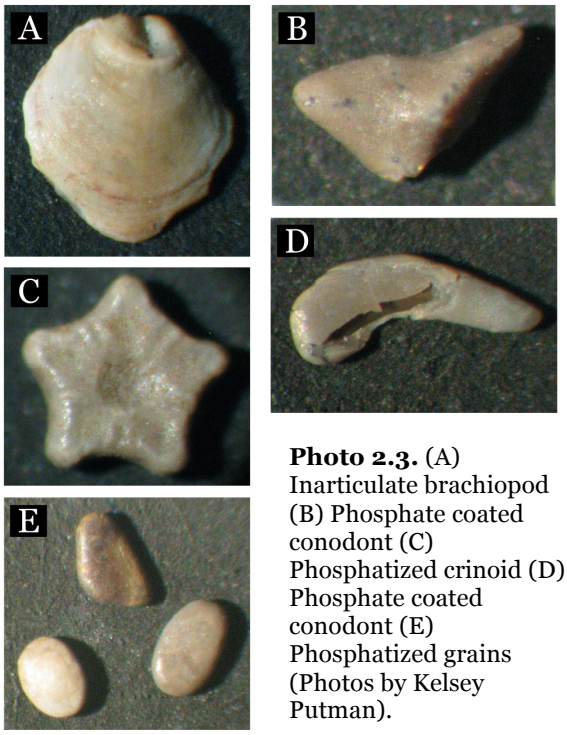

Photo 2.3. (A) Inarticulate brachiopod (B) Phosphate coated conodont (C) Phosphatized crinoid (D) Phosphate coated conodont (E) Phosphatized grains (Photos by Kelsey Putman).

and little thermal alteration (Photo 2.2.). Other grains picked for analysis included phosphatized crinoids, phosphate coated grains and inarticulate brachiopods (Photo 2.3.).

Because conodont elements are small, it was necessary to pick 30-60 elements per sample in order to have enough mass ($\geq$ 250 μg) to yield sufficient Ag_3PO_4 crystals for the mass spectrometer analysis described below.

2.3.2.4. *Generation of Ag_3PO_4*

In order to generate Ag_3PO_4, a modified version of the technique described by O'Neil et al. (1994) was used. Typically 250 - 900 μg of species-specific conodonts or other phosphate grains were weighed out on a balance and bleached overnight in 1 mL of 4-6% NaOCl in a 1.5 mL microcentrifuge tube. The samples were then rinsed 3 times with deionized H_2O and dried in an oven at 50°C. After samples have been dried, 100 μL of 0.5 M nitric acid was added to each dried sample and left overnight or until the solids were dissolved. In order to increase the pH 100 μL of 0.5 M KOH was added. Next, 200 μL of 0.01 g/mL (0.17 M) KF was added to remove Ca^{2+}. The samples were then swirled in a Vortex Genie and left standing until any reaction that occurred was complete.

Samples were then centrifuged and the supernatant was transferred to a clean, low binding Eppendorf micro centrifuge tube while leaving behind any insoluble material such as Ca salts. To insure that the sample came back to a low pH, 25 μL of 0.5 M HNO_3 was added. It was noted that by increasing the pH

before adding Ag^+, the tendency for the present Ag_3PO_4 to "crash" out of solution and form tiny and unusable silver phosphate crystals was greatly diminished. So, next, 150 µL of 2 M NH_4OH was added. Finally, 150 µL of silver solution (0.4 M $AgNO_3$, 0.7 M NH_4NO_3) was added and ammonia was able to de-gas slowly by leaving the micro centrifuge tube caps open sat overnight in the oven set at 50°C. Once crystals of silver phosphate formed in the vials, deionized H_2O was added to cover any exposed crystals that had grown. The vials were then briefly sonicated to dislodge crystals clinging to the walls. The supernatant was pipetted from each sample, and the remaining silver phosphate crystals were rinsed 3-5 times with 1 mL of water. Samples were dried in a 50°C oven, weighed, and transferred into Ag capsules for analysis.

2.3.2.5. *Mass Spectrometry Analysis*

Silver phosphate crystals were weighed on a balance and the crystals were transferred to silver capsules. These capsules were crushed into small cubes (3.3 x 5mm) and placed in a desiccator until ready to analyze. For analysis, each sample was placed into a well of an automated carousel and then dropped into the TC/EA reactor and decomposed at 1400°C (following procedures in Bassett, 2007). Standards of Benzoic Acid and an ACROS silver phosphate were analyzed concurrently to allow for correction for machine drift between runs and to monitor analytical precision.

Each sample was decomposed in the reactor which released oxygen when the phosphate-oxygen bond was broken by pyrolysis (LaPorte et al. 2009). The oxygen combined with C in the furnace to form CO which was carried out of the reactor and through the Thermo Finnigan DeltaPlus GC-IRMS using He as the carrier gas (LaPorte et al. 2009; Bassett, 2007). The isotopic composition of the CO was measured by continuous flow mass spectrometry relative to a reference gas of known isotopic composition. Results are reported relative to the Vienna Standard Mean Ocean Water (V-SMOW) in delta notation. Because samples were measured over a two-year period, every individual run had its own benzoic acid standard to which the data was corrected by. Those averages for each run may be found in the Appendix A-C. For simplicity, the average of the 41 benzoic acid standards is reported here as 23.88 ‰ (the average of the benzoic acid), and the standard deviation is 0.19 (the averaged standard deviations).

2.3.3. $\varepsilon_{Nd(t)}$ *Data Collection*

The inarticulate brachiopod, *Leptobolus* was picked from the same sand sized insoluble sediment residue as the conodonts for the $\delta^{18}O$ thermometry portion of the study. Both clean fragments and whole shell brachiopod samples were picked from Webber Quarry samples, weighing between 500 μg to 1 mg. These samples were then sent to the University of Florida for $\varepsilon_{Nd(t)}$ analysis.

2.3.3.1. *Sample Preparation*

The following reported lab procedure has been modified from Jiménez Berrocoso et al. (2010). The Nd ratios of the brachiopods were analyzed at the University of Florida. Separates were dissolved in 200 μl aqua regia to remove any organic matter. Samples were then dried and redissolved in 1.6 N HCl. The samples were then processed using two cation exchange columns; the first column separated bulk Rare Earth Elements from any other present cations using Mitsubishi resin and HCl as an eluent. Bulk REE was then cut and dried and loaded onto small Teflon column packed with Ln Spec™ resin. Neodymium was the eluted with 0.25 N HCl.

The neodymium isotopes were then measured on a Nu multi-collector inductively-coupled mass spectrometer (MC-ICP-MS) at the University of Florida. The fractions of neodymium were then dried and redissolved in 0.3 mL of 2% optima HNO_3. All samples were analyzed using a desolvating nebulizer (DS-100). Samples were analyzed using a time-resolved analysis (TRA) method (Kamenov et al., 2008). Baseline was measured for 30 seconds prior to the introduction of the sample to the electrostatic analyzer (ESA) deflection of the ion beam. All ratios were corrected for mass fractionation using $^{146}NdO/^{144}NdO = 0.7219$.

CHAPTER 3: Lithologic Descriptions and Stratigraphic Overview

The Dubuque Formation, the lower of the two formations discussed in this project, can be characterized as a fossil-rich wackestone to packstone with minor dolomitization. The Dubuque is part of the Galena group, and in most literature is not broken down into separate Members. Samples in this study, were all collected from the upper portions of the Dubuque Formation.

The Maquoketa Formation is subdivided into three members; this study focuses on the lowermost member, the Elgin Member. The Elgin Member generally is composed of shale with minor carbonate inter beds; the carbonate beds become increasingly dominant to the north in Minnesota and northern Iowa. The contact between the formations is recognizable by a phosphate horizon and associated sculpted hardgrounds. This phosphate horizon has been mapped east into Indiana, south into northern Missouri, and as far north as Allamakee County, Iowa (Witzke, 1980). This horizon does not extend into Minnesota.

Of the seven locations, three yielded samples containing enough conodont and brachiopod material to yield $\delta^{18}O$ data; only one of the three sites was sampled for $\varepsilon_{Nd(t)}$ analyses. These three localities were grouped into what we identified as southern, central, and northern regions. In this section, lithologic and stratigraphic discussions are presented for these three regions. The South Williams Core did not yield sufficient phosphatic material for $\varepsilon_{Nd(t)}$ or $\delta^{18}O$

analyses and did not have similar lithologies as other locals and has been excluded from regional grouping and descriptions. This core's lithologic descriptions are listed first.

3.1. South Williams Core

Dubuque Formation

The lithologic transition between the Dubuque and Maquoketa was sampled from a core in Louisa Co., IA (Photo 3.1.) The Dubuque Formation varies here from a grey to tan argillaceous dolomite with beds ranging from 5-8 mm thick (Witzke and Bunker, 1996). White-creamy colored calcite filled vugs range in size from 1- 15 mm and occupy 2-5% of the matrix. Shale stringers common and range from 1-4 mm thick, with associated stylolites.

Photo 3.1. The South Williams Core from southern Iowa (Photo Ken MacLeod).

Elgin Member of the Maquoketa Formation

The rocks in the Elgin Member of this section vary between phosphatic shales, vuggy argillaceous dolomites and dolomitic shales. The basal Elgin Member varies between phosphorites and phosphatic dolomite that sits on a sculpted hardground (Witzke and Bunker, 1996). The hardground and phosphorite is commonly used as the characteristic feature that separates the Dubuque Formation and Maquoketa Formation.

Photo 3.2. The sampled section of the Dubuque Formation in the Webber Quarry, IA (Photo by Ken MacLeod).

3.2. Southern Region (Webber Quarry, Big Springs Core, Graf, Highway 20)

Dubuque Formation

The Dubuque Formation at the Webber Quarry (Photo 3.2.) is characterized as a trilobite, brachiopod, echinoderm wackestone that has

occasional vertical burrows. Dark shale stringers can be found in the formation and form locally recessive units (Raatz and Ludvigson, 1996). The massive wackestone beds toward the bottom of the section are replaced progressively to thinner, highly fractured dolomitic beds. Linguloid brachiopods are common throughout the measured section.

Elgin Member of the Maquoketa Formation

The Graf location is the type locality for the Maquoketa Formation (James, 1890) and contains four specific layers of nautiloid cephalopod coquinas. Even though this locality has been identified as the type locality, the distinctive nautiloid coquinas are not continuous throughout the Maquoketa Formation. In the Webber Quarry, which is considered more "typical" (Raatz and Ludgivson, 1996), the Elgin Member is believed to represent a transition between the southern shale deposits and northern carbonates (Raatz and Ludvigson, 1996). The basal Elgin is represented by the phosphatic hardground that is characteristic for this region

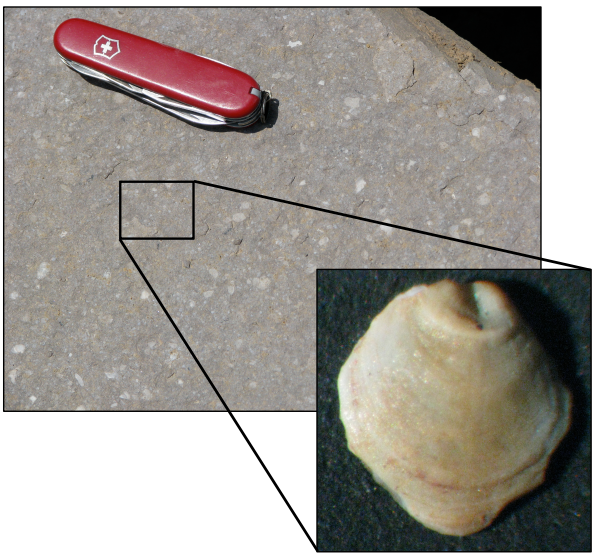

Photo 3.3. An example of the inarticulate brachiopod Leptobolus in a hand sample of Maquoketa shale (Photos by Ken MacLeod and Kelsey Putman).

that also marks the contact between the two formations. This phosphate horizon contains abundant diminutive molluscs as well as other diminutive hardy benthic fauna (Ladd, 1929). A dark brown shale overlies the phosphate horizon containing abundant graptolites and linguiloid brachiopods (Photo 3.3.). Thin dolomite beds are interspersed within brown shales which grade upwards to more massive dolomites containing shales.

3.3. Central Region (Postville Roadcut and Quarry)

Dubuque Formation

The Dubuque Formation at the Postville Roadcut (Photo 3.4.) is characterized by trilobite, brachiopod, echinoderm wackestone that has occasional storm event packstones and burrows (Raatz and Ludvigson, 1996). The matrix is light buff micrite with lenses of dark shale. Interspersed in the limestone are dolomitic horizons that contain blocky dolomitic rhombs. Calcite cement infillings are common in vugs as well as void fillings of brachiopods and ostracods (Raatz and Ludvigson, 1996).

Photo 3.4. The sampled section of Dubuque Formation at the Postville Roadcut, IA (Photo by Kelsey Putman)

Elgin Member of the Maquoketa Formation

The contact between the Elgin and Dubuque is represented by condensed phosphatic hardgrounds. One to three hardgrounds have been identified at this location, they contain intermixed phosphate pelloids, ooids, iron sulfides, and burrows that form poorly sorted phosphatic grain stone (Raatz and Ludvigson, 1996). This location also contains abundant diminutive fauna distribution as follows: 2752 Mollusca, 941 Brachiopoda, 454 Arthopoda, 348 Echinodermata, 48 Protochordata, 30 Hyolitha, 8 Cnidaria, and 7 Bryozoa; all counted from a random sample of the phosphate horizon to determine faunal diversity and abundance in a previous study (Putman et al., 2008). Phosphatic concretions usually 1-2mm in diameter are abundant in the phosphate horizon. Three dimensionally preserved graptolites can be seen in the phosphate horizon, as well

Photo 3.5. A view of the Postville Quarry vertical face. Previous field work allowed for sampling when a bench was present on the uppermost Dubuque Formation (Photo by Kelsey Putman).

as minor 3-D graptolites in a brown shale layer overlying the phosphate horizon. The phosphate horizon of the Postville Quarry was sampled initially in the summer of 2004 when a significant ledge in the quarry separated the lower Dubuque from the overlying Maquoketa Formation. Upon return in summer of 2010, the ledge had been removed, preventing further sampling of the Maquoketa

Formation (Photo. 3.5.).

3.4. Northern Region (Rifle Hill)

Dubuque Formation

The Dubuque Formation is a trilobite, brachiopod, echinoderm wackestone to packstone with horizontal and vertical burrows (Raatz and Ludvigson, 1996). The abundance of dolomite increases up section, as does the presence of wavy bedding. The lower Dubuque Formation has a micritic matrix, and calcite cements are present as infilling of voids left from dissolved small brachiopods

Photo 3.6. Example of the Dubuque Formation at the Rifle Hill Roadcut, MN (Photo by Ken MacLeod).

and mollusk shells. Sulfide cubes (100 μm in size) and sulfide replacement of sponge spicules are locally abundant. Local shaley laminations intersperse most dolomite and micrite beds (Photo 3.6.).

Elgin Member

The Elgin Member, sampled at the Rifle Hill Roadcut and Quarry is characterized by an echinoderm, trilobite, graptolite, brachiopod mudstone to wackestone that has abundant burrowing (Raatz and Ludvigson, 1996). The phosphatic hardground marker bed that is present in the central and southern locations is absent at Rifle Hill (Photo 3.7.), and the Dubuque-Maquoketa Formational contact is recognized by biological markers, most notably the first appearance of graptolites (Raatz and Ludvigson, 1996). Based on previously measured sections at Rifle Hill by Witzke, the contact between the two formations is placed at a brachiopod packstone bed.

Photo 3.7. Comparison of the contact between the Dubuque and Maquoketa Formations. (A) Contact at the Rifle Hill, MN location, marked by a brachiopod packstone bed. (B) Contact at the Postville Quarry, IA location marked by the phosphate bed (Photos by Ken MacLeod and Norlene Emerson).

CHAPTER 4. Results and Implications for Paleoceanography

4.1. Results for $\delta^{18}O$ Conodont Paleothermometry

Out of the seven sampled locations, only the Webber Quarry, Postville, and Rifle Hill locations yielded enough conodonts or brachiopods to analyze $\delta^{18}O$ in bioapatite through the section. The South Williams and Big Springs core, Graf Road and Highway 20 localities produced few to no conodonts so that running either bulk or species specific separates was not possible. The following section reporting results and the subsequent discussion will be referring to $\delta^{18}O$ data as "per mil" values, and not estimated temperatures. See Appendix for estimated temperatures.

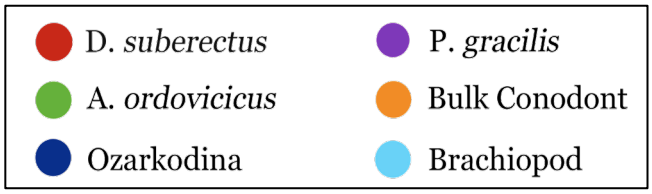

Key for figures 4.1. 4.2., 4.3.

4.1.1. *Brachiopod Data*

The phosphatic inarticulate brachiopod, *Leptobolus*, was run to track potential diagenetic artifacts within, and among sections (Fig. 4.1.). I found fairly good agreement in $\delta^{18}O$ values among brachiopod samples within each section,

but large differences exist in the average values for brachiopod separates among sections. In the Webber Quarry, brachiopods have low $\delta^{18}O$ values, varying between 17.9 ‰ to 16.1 ‰. The Postville section brachiopods had low $\delta^{18}O$ values as well, varying between 18.5 ‰ to 17.6 ‰. The Rifle Hill section returned $\delta^{18}O$ values ranging between 20.1 ‰ to 19.3 ‰ (Fig. 4.1.).

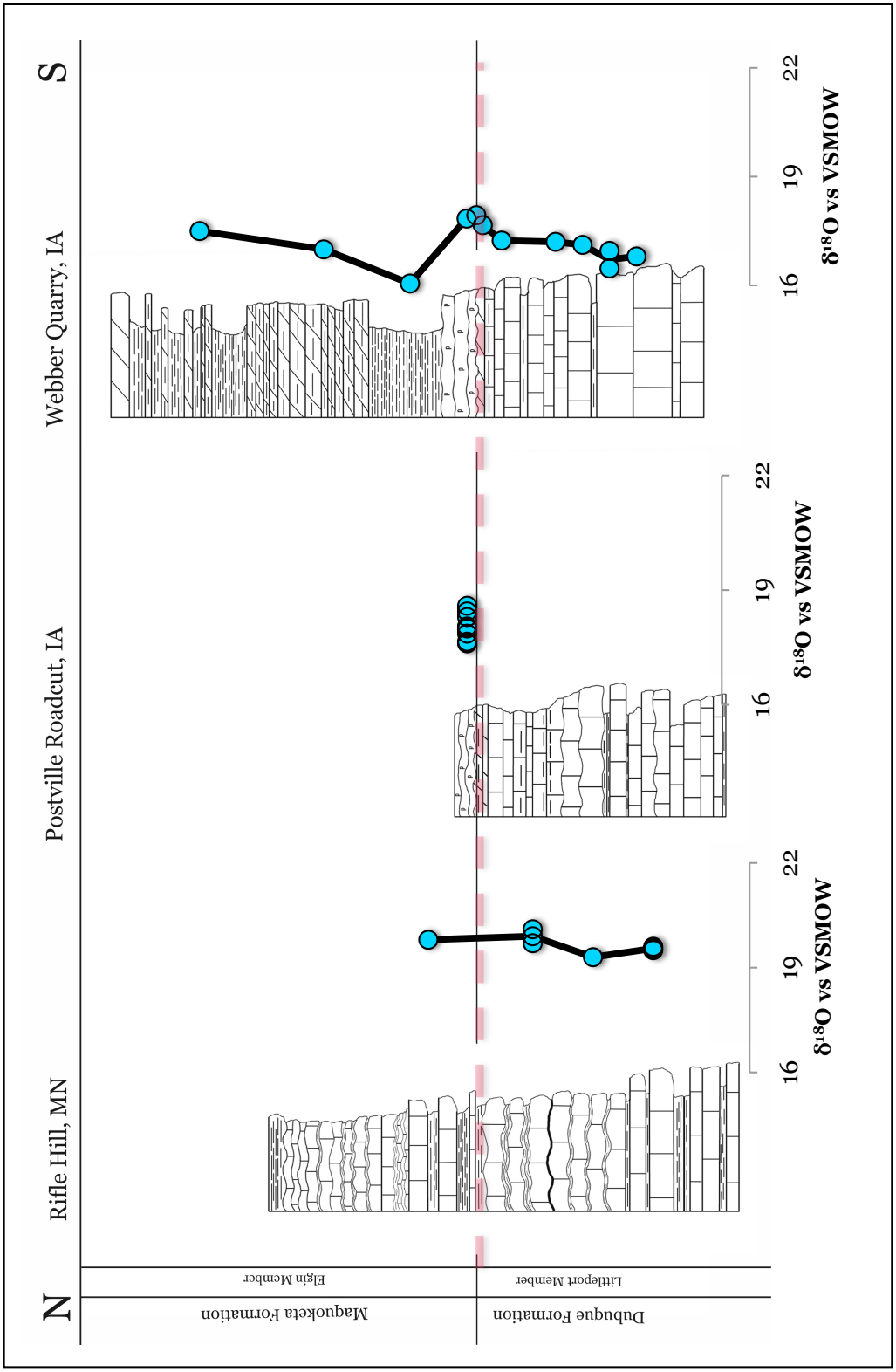

Figure 4.1. Brachiopod $\delta^{18}O$ values plotted next to stratigraphic columns of each local.

4.1.2. *Species Specific Conodont Separates*

The most abundant species from the three localities is *Drepanoistodus suberectus*, which was present across the lithologic transition in all three sections. *D. suberectus* samples yielded data that had both good agreement within each section, and among sections. *D. suberectus* averaged 18.9 ‰ in the Webber Quarry, an average of 18.6 ‰ in the Postville section, and 18.7 ‰ in the Rifle Hill section. No excursions or consistent trends are present in the *D. suberectus* curves.

Other species specific separates included, *Ozarkodina* spp., *Amorphognathus ordovicicus*, and *Panderodus gracilis*. *Ozarkodina* spp. and *A. ordovicicus* were only present in enough abundance to analyze at the Postville locality. At that location, *Ozarkodina* spp. and *A. ordovicicus* curves tended to plot to the right of (higher $\delta^{18}O$ values) the *D. suberectus* curve, in the 18.5 to 19.5 ‰ range. In contrast, the *P. gracilis* curve seen in the Postville locality plots to the left of the *D. suberectus* curve for two of the three samples. Similarly, the one *P. gracilis* sample in the Webber Quarry also plots to the left of the *D. suberectus* curve. In both of these instances, an ~1 ‰ offset occurs between the *P. gracilis* and *D. suberectus* points.

The bulk conodont curve tends to parallel, but be slightly higher than, the *D. suberectus* curves in both the Webber Quarry and Postville sections (Fig. 4.3.). The bulk conodont curve plots between 20.1 ‰ to 18.7 ‰ at the Webber Quarry location, where the *D. suberectus* data plots between 20.1 ‰ to 17.3 ‰. The bulk

conodont curve plots between 19.9 ‰ to 18.9 ‰ at the Postville location, whereas the *D. suberectus* data plots between 19.2 ‰ to 17.9 ‰.

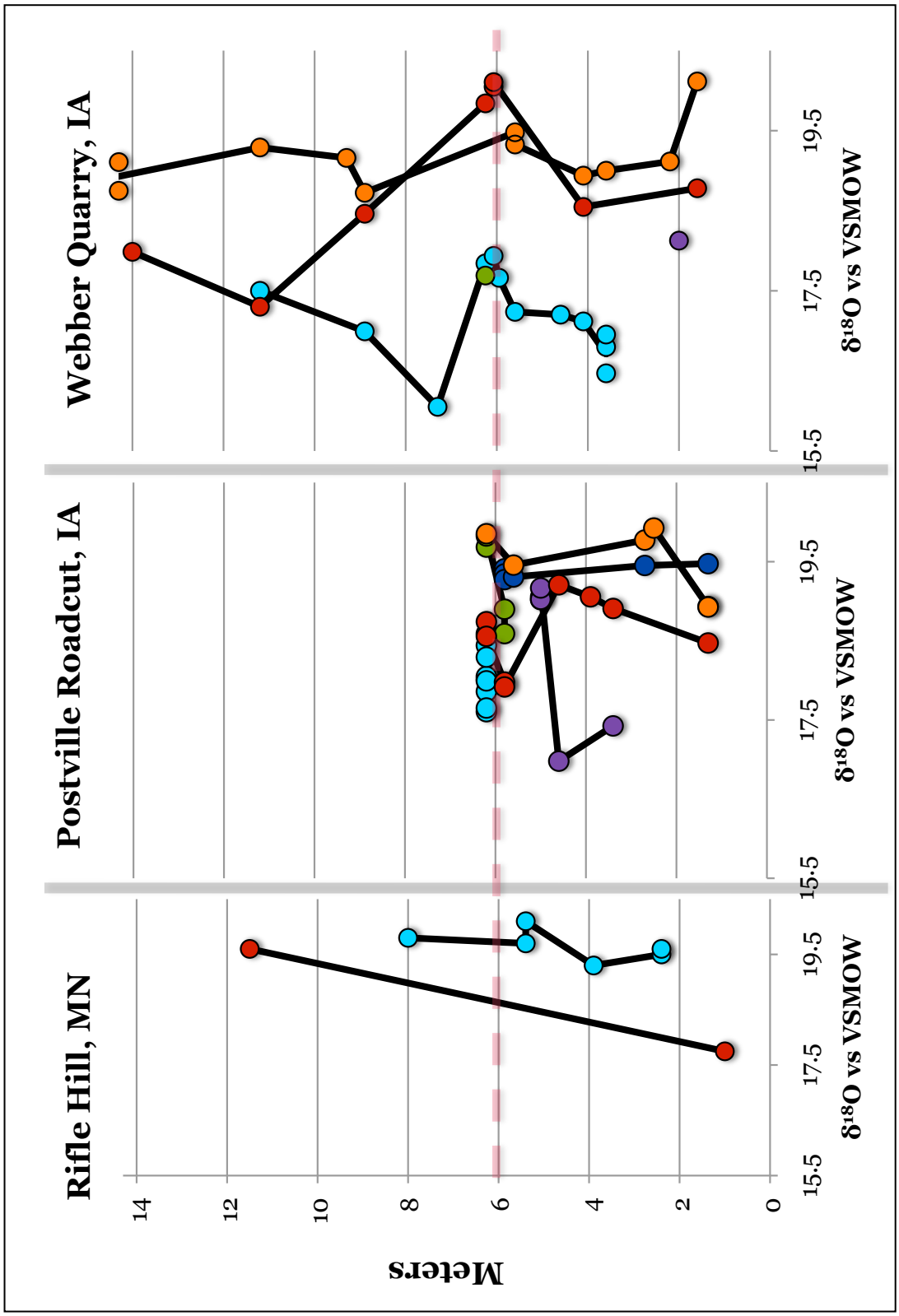

Figure 4.2. Compilation of $\delta^{18}O$ data for all three localities, with Rifle Hill to the North and Webber Quarry to the South.

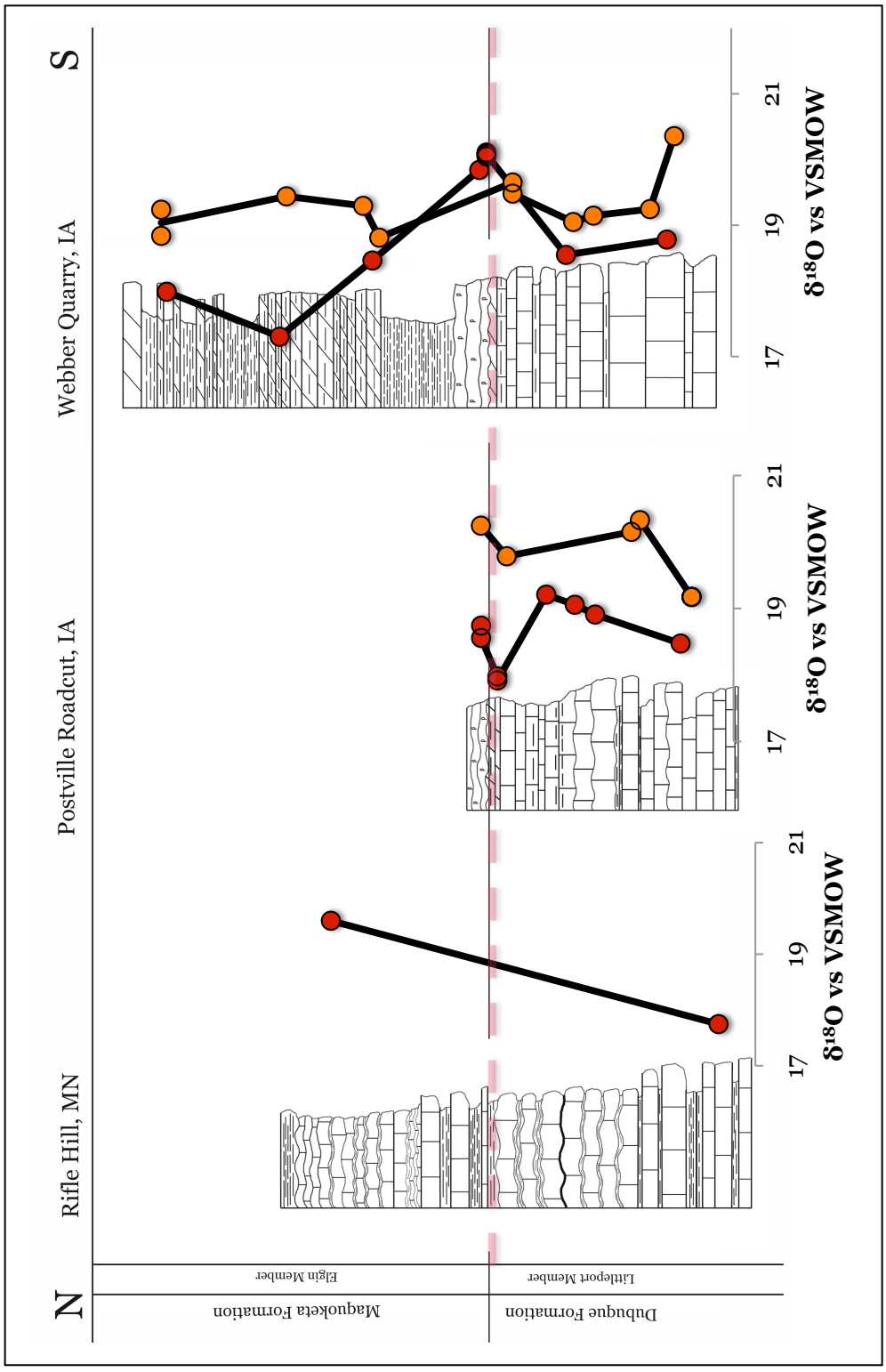

Figure 4.3. $\delta^{18}O$ data for both *Drepanoistodus suberectus* and bulk conodont curves plotted next to stratigraphic sections.

4.1.3. *Phosphatized Grains*

Because so many previous models had incorporated the concept of cool, nutrient rich water upwelling and depositing the phosphorite horizon at the basal Maquoketa, these phosphatized and coated grains were tested to determine if their $\delta^{18}O$ value supported such a model. These grains were tested at the phosphate horizon at the Postville Quarry to also aid in tracking diagenetic alteration at this horizon. The phosphatized and coated grains were found to have at least an 0.5 to 1 ‰ variability within one sample (phosphatized crinoids: 16.7 ‰ to 17.8 ‰; phosphate grains: 17.7 ‰ to 18.2 ‰).

4.2. Results for $\varepsilon_{Nd(t)}$ data

Brachiopod $\varepsilon_{Nd(t)}$ data was collected from the phosphatic inarticulate brachiopod, *Leptobolus* (Photo 5.1.) from the Webber Quarry. Because this taxon was abundant at this locality, samples were taken from each bulk rock sample resulting in a nearly 1-meter resolution for $\varepsilon_{Nd(t)}$ samples through the Webber Quarry.

Photo 5.1. The inarticulate brachiopod, *Leptobolus* (Photo by Kelsey Putman

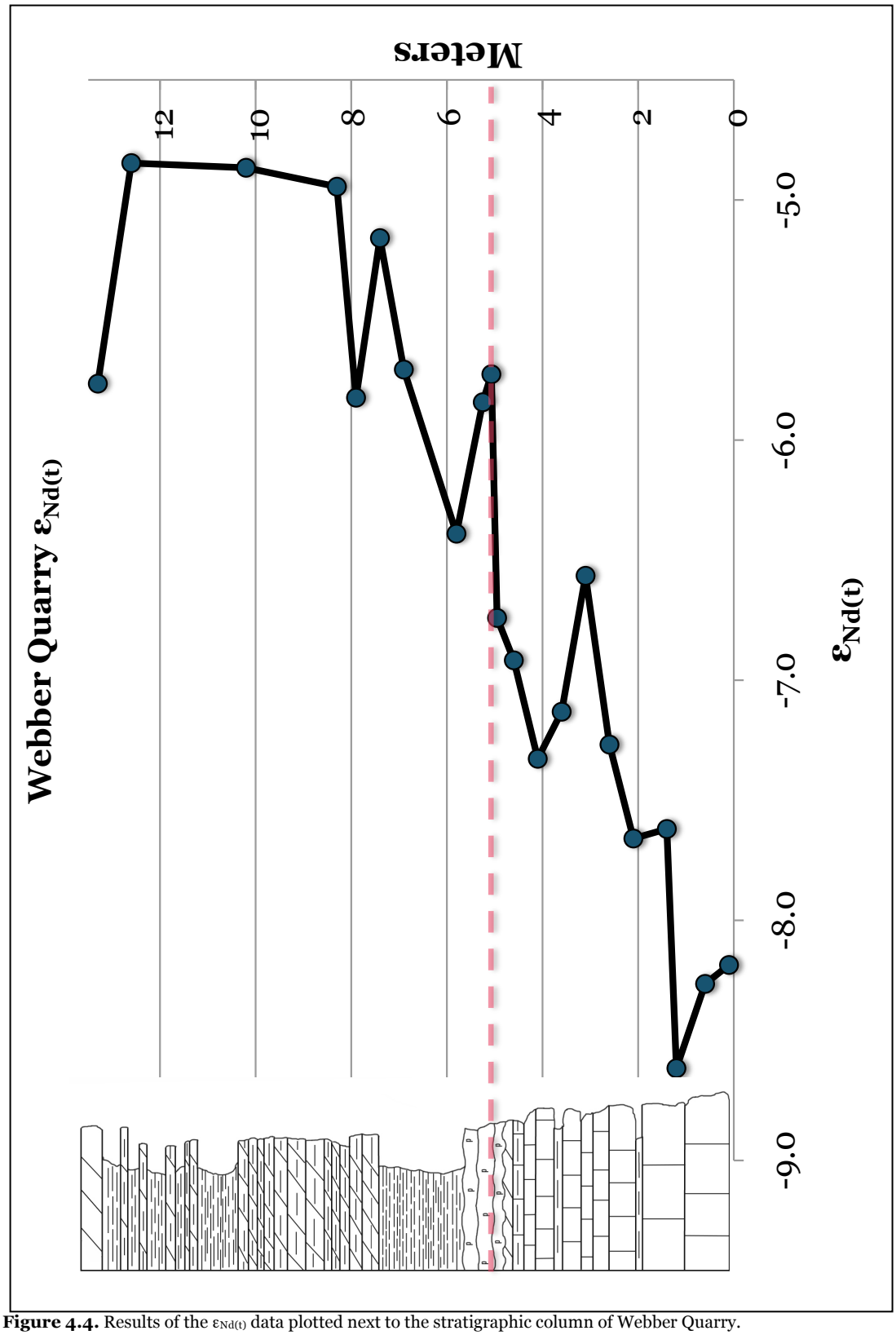

Figure 4.4. Results of the $\varepsilon_{Nd(t)}$ data plotted next to the stratigraphic column of Webber Quarry.

As seen in the figure (4.4.), a steady increase of $\varepsilon_{Nd(t)}$ values persists across the formational contact. The Dubuque Formation $\varepsilon_{Nd(t)}$ values ranges between -8.1 to -6.9, where the Maquoketa Formation $\varepsilon_{Nd(t)}$ values range from -6.7 to -4.8. The $\varepsilon_{Nd(t)}$ values between the two formations do not overlap and show a steady increase through time.

4.3. Implications for Paleoceanography

4.3.1. *$\delta^{18}O$ Data Interpretation*

The $\delta^{18}O$ values did not vary across the formational contact of the Dubuque and Maquoketa Formations, contrary to previous models which invoked upwelling of cool nutrient rich water at the phosphate interval. Further research on the phosphatic inarticulate brachiopods was done to determine if paleocirculation changed across the lithologic contact, or stayed consistent through time. Yet, in the paleothermometry portion of this study, the brachiopod *Leptobolus* used to track diagenetic alteration within and among sections also proved to be a valuable set of data for this study. I found that brachiopod $\delta^{18}O$ data had good agreement within each section, yet had poor agreement among sections. These samples were used as a proxy for diagenetic alteration, and the consistent differences among sections indicate the extent of diagenetic alteration varied along the sampling transect. Good agreement of the brachiopod would indicate less diagenetic alteration across the sampling transect. The Webber

Quarry and Postville sections appeared to have the most alteration, and the Rifle Hill section is apparently less altered. The highest $\delta^{18}O$ values for each location of the conodont *D. suberectus* range between 19.2 ‰ to 20.1 ‰, while the lowest $\delta^{18}O$ values range between 17.3 ‰ to 17.7 ‰. Little disagreement exists among the *D. suberectus* conodont separates based on the $\delta^{18}O$ data. These results probably indicate that the phosphatic inarticulate brachiopod is more susceptible to alteration than the bioapatitic conodonts. This interpretation is consistent with earlier studies (Wenzel et al., 2000; Joachimski and Buggisch, 2002; Bassett et al., 2007).

The $\delta^{18}O$ data indicated no significant cooling across the contact of the Dubuque and Maquoketa Formations. There is only a small excursion at the contact between the two formations, observed in the *D. suberectus* and bulk conodont curves. The phosphatized and coated grains sampled at the phosphate horizon at the Postville Quarry did not reflect the same excursion as the conodont *D. suberectus*. Instead the phosphatized and coated grains had $\delta^{18}O$ values that were lower than *D. suberectus*. Because models have suggested upwelling of cool water during the deposition of the phosphate horizon, an excursion of $\delta^{18}O$ should have been seen at the contact. It is unlikely that the low $\delta^{18}O$ values preserved in the phosphatized and coated grains are providing a value indicative of bottom water temperatures. Thus, $\delta^{18}O$ values provide no additional support for upwelling of cool water, sourced either from the open ocean or the Sebree Trough. Instead, it is possible that the phosphate rinds coating many of these grains are recording a diagenetic signature.

The trend of the *D. suberectus* and bulk conodont curves tracking together in the Webber Quarry and Postville sections is likely due to the composition of the bulk conodont samples. Bulk conodont samples were typically run when there was not enough of one particular species to run as a separate. While many species were included in bulk analyses, *D. suberectus* was the most abundant species throughout the whole study and tended to dominate the bulk separates. The most common additions (which are also represented by relatively large elements) were *Ozarkodina* spp. and *A. ordovicicus*. Since both of these taxa plot to the right of the *D. suberectus* curve in the Postville section, they should shift the bulk results to slightly higher values than for *D. suberectus*, exactly the pattern observed.

This tendency for species to show consistent offsets within and among sections supports research done by Leslie and Bergstrom (1997) and Leslie (2009) on conodont biofacies. Leslie (2009) found through cluster analysis that certain conodont species tended to occur within discreet facies suggesting preference among taxa for different living environments. The conodonts *D. suberectus* and *P. gracilis* likely lived in surface waters (Leslie, 2009), which should be relatively warm and this prediction is supported in this study as these two species consistently have the lowest $\delta^{18}O$ values of all the conodont species. It has also been suggested by Leslie (2009) that the conodont *A. ordovicicus* lived at or near the sea floor where temperatures might be cooler. This model is also supported by this study as the *A. ordovicicus* conodont plots to the right of *D.*

suberectus and *P. gracilis*. In addition, *A. ordovicicus* was also the most abundant localized around the contact of the two formations, during a time when water depth was the highest due to sea level highstand. *Ozarkodina* was not included in Leslie (2009) study, but the *Ozarkodina* curves tracks with the *A. ordovicicus* curve, which supports an interpretation that these conodonts also preferred similar living conditions as *A. ordovicicus*.

Based on the $\delta^{18}O$ data, there appears to be no long-term temperature trends through the Dubuque and Maquoketa Formations. Apart from the minor excursion in the *D. suberectus* curve, which is interpreted to be from upwelling, there is no evidence for climate change, or circulation change across the lithological contact.

4.3.2. *Brachiopod $\varepsilon_{Nd(t)}$ Data Interpretation*

The progressive increase in $\varepsilon_{Nd(t)}$ values beginning below and continuing across the Dubuque/Maquoketa contact suggests an increasing influence of Taconic derived and/or open ocean waters during the interval studied. The $\varepsilon_{Nd(t)}$ values for the Dubuque Formation (-8.2 to -6.5) do not overlap those of the Maquoketa Formation (-5.7 to -4.8), and steadily increase through the 14-meter section in Webber Quarry. The 14 meters sampled in this study highlight the transgressive-regressive sub cycle that has been interpreted for this region (Raatz and Ludvigson, 1996). Values consistent with Midcontinent $\varepsilon_{Nd(t)}$ values identified by Holmden et al., (1998) at -15.4 +/- 2.6 were not observed in any of our samples. It is likely low values should be present in the Dubuque based on the data from

Holmden et al., 1998 from the earlier time slice of the Mohawkian sea, but lower in the section and beyond the 14 meters sampled in this study. It is possible that for the time slice sampled for this study, the effects of the transgression are dominant, where Taconic and/or open ocean sourced water with lower $\varepsilon_{Nd(t)}$ values were flowing into the region and replacing a water mass imprinted with

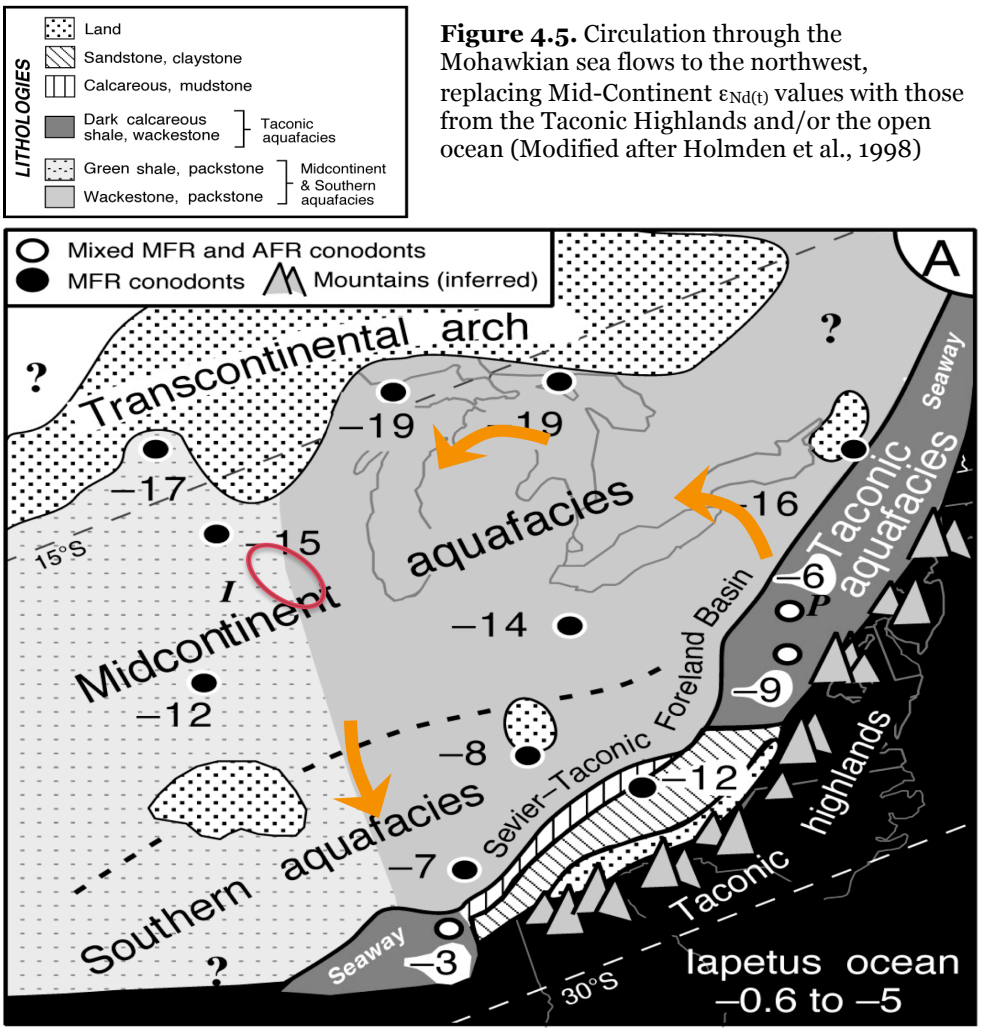

Figure 4.5. Circulation through the Mohawkian sea flows to the northwest, replacing Mid-Continent $\varepsilon_{Nd(t)}$ values with those from the Taconic Highlands and/or the open ocean (Modified after Holmden et al., 1998)

the Midcontinent $\varepsilon_{Nd(t)}$ values. Taconic $\varepsilon_{Nd(t)}$ values identified by Holmden et al., (1998) at -7.5 +/- 2.3 are well within the range of the values we report for the Dubuque Formation. Open ocean values were also identified by Holmden et al.,

(1998) that range between -0.6 to -5 just overlapping on the range of values we report for samples from the Maquoketa Formation.

The data suggests that increased runoff from the Taconic Highlands and/or open ocean sourced water was circulating into the Midcontinent during the deposition of the Dubuque and Maquoketa Formations (Fig. 4.5). The Taconic Highlands at the time were still a young island arc system and freshwater run off from this region of high relief would have been imprinted with $\varepsilon_{Nd(t)}$ values reflective of young crystalline igneous rock. This Taconic sourced water mass then flowed into the Midcontinent, which had $\varepsilon_{Nd(t)}$ values reflective of the weathering Precambrian Shield and Transcontinental Arch to the paleonorth. During the deposition of the Maquoketa Formation, it is possible that open ocean water flowing into the Midcontinent via the Sebree Trough was also influencing the region and is reflective of the increased $\varepsilon_{Nd(t)}$ values seen in the Maquoketa Formation.

CHAPTER 5. Summary and Conclusion

By utilizing both $\delta^{18}O$ and $\varepsilon_{Nd(t)}$ values, I suggest that there was no significant change in temperature across the Dubuque-Maquoketa Formational contact and a shift from Mid-continent $\varepsilon_{Nd(t)}$ values to Taconic and/or open ocean $\varepsilon_{Nd(t)}$ values coincides with the highstand of a transgressive-regressive subcycle. The $\delta^{18}O$ values also indicate niche partitioning and preferential living conditions

for different conodont taxa. Because there are no significant changes in the $\delta^{18}O$ values across the contact, the data from this study alters previous interpretations for cool water upwelling, as well as an incursion of cool open ocean water impinging on the shallow carbonate ramp. Data from phosphatized grains and coated grains at the phosphate horizon yielded low $\delta^{18}O$ values suggesting unreasonably high bottom water temperatures and instead are interpreted as indicating a possible secondary phosphate crystal growth, unrelated to upwelling. The data in this study does not provide support for upwelling. The data and subsequent interpretations best describe the lithologic transition between the Dubuque and Maquoketa Formation to be the result of circulation changes, and not from climate changes.

The $\delta^{18}O$ data from the phosphatic inarticulate brachiopods does suggest that there was diagenetic alteration among sections and served as an appropriate material to test for diagenetic artifacts. However, the $\delta^{18}O$ data from the conodont samples does not vary among sections, which further supports the claim that conodont $\delta^{18}O$ values are more stable and less susceptible to diagenetic alteration.

Future research should focus on increasing the sampled interval to extend further above and below the contact in hopes of discovering the initiation of the transgressive event, and end of the regression by means of $\varepsilon_{Nd(t)}$. Tracking the contact further south, and across the Sebree Trough would also be beneficial to establish boundaries on regional aquafacies.

Appendix

A. $\delta^{18}O$ Webber Quarry Data Table

sample	formation	meters above base	conodont*/ grain type	$\delta^{18}O$ V-SMOW (corrected)	group**	estimated t°C***
WQ- M10 bulk 1	Maquoketa	13.3	*Oz; Ds; Ph*	**18.7**	3	26.4
WQ- M10 bulk 2	Maquoketa	13.3	*Oz; Ds; Ph*	**19.1**	3	24.9
WQ-M10 Ds	Maquoketa	13.3	*Drepanoistodus suberectus*	**17.4**	2	32.2
WQ- M7 bulk	Maquoketa	10.2	*Ph; Ao; Ds*	**19.3**	3	24.1
WQ- M7 Ds	Maquoketa	10.2	*Drepanoistodus suberectus*	**17.3**	3	32.7
WQ- M6 bulk	Maquoketa	8.3	*Oz; Ph*	**19.2**	3	24.7
WQ-M5 Ds	Maquoketa	7.9	*Drepanoistodus suberectus*	**17.9**	2	30.1
WQ- M5 Brach	Maquoketa	7.9	*Leptobolus, brachiopod*	**17.0**	3	34
WQ- M5 bulk	Maquoketa	7.9	*Oz; Ds*	**18.7**	3	26.5
WQ-M1 brach	Maquoketa	5.8	*Leptobolus, brachiopod*	**15**	2	42.6
WQ- P2 Ao	Phosphate Horizon	5.2	*Amorphognathus ordovicicus*	**17.7**	3	31
WQ- P2 Brach	Phosphate Horizon	5.2	*Leptobolus, brachiopod*	**17.8**	3	30.3
WQ- P2 Ds	Phosphate Horizon	5.2	*Drepanoistodus suberectus*	**19.8**	3	21.7
WQ- P1 Brach	Phosphate Horizon	5.1	*Leptobolus, brachiopod*	**17.9**	3	29.9
WQ- P1 DS 1	Phosphate Horizon	5.1	*Drepanoistodus suberectus*	**20.0**	3	20.8
WQ- P1 DS 2	Phosphate Horizon	5.1	*Drepanoistodus suberectus*	**20.1**	3	20.6
WQ- P1 DS 4	Phosphate Horizon	5.1	*Drepanoistodus suberectus*	**20.1**	3	20.7
WQ- P1 DS 5	Phosphate Horizon	5.1	*Drepanoistodus suberectus*	**19.0**	3	25.3
WQ- D11 Brach	Dubuque	4.9	*Leptobolus, brachiopod*	**17.7**	3	31.1
WQ- D10 Brach	Dubuque	4.6	*Leptobolus, brachiopod*	**17.2**	3	32.9
WQ- D10 bulk 1	Dubuque	4.6	*Oz; Pg; Ao*	**19.5**	3	23.3
WQ- D10 bulk 2	Dubuque	4.6	*Oz; Pg; Ao*	**19.3**	3	23.9
WQ- D8 Brach	Dubuque	3.6	*Leptobolus, brachiopod*	**17.2**	3	33.1
WQ- D7 Brach	Dubuque	3.1	*Leptobolus, brachiopod*	**17.1**	3	33.4
WQ- D7 bulk	Dubuque	3.1	*Pg; Oz; Ds*	**18.9**	3	25.6
WQ- D7 Ds 1	Dubuque	3.1	*Drepanoistodus suberectus*	**18.5**	3	27.3
WQ- D6 Brach 1	Dubuque	2.6	*Leptobolus, brachiopod*	**17.0**	3	34.1
WQ- D6 bulk 1	Dubuque	2.6	*Ds; Pg; Be*	**18.7**	3	26.5
WQ- D6 bulk 2	Dubuque	2.6	*Ds; Pg; Be*	**19.8**	3	21.8
WQ- D6 Brach	Dubuque	2.6	*Leptobolus, brachiopod*	**16.5**	3	36.2

WQ- D5 brach	Dubuque	2.1	*Leptobolus, brachiopod*	**16.8**	3	34.8
WQ- D3 bulk	Dubuque	1.2	*Pg; Oz*	**19.1**	3	24.9
WQ- D2 bulk	Dubuque	0.6	*Pg; Ds; Oz*	**20.1**	3	20.6
WQ- D2 Ds	Dubuque	0.6	*Drepanoistodus suberectus*	**18.8**	3	26.3
WQ-D1 P	Dubuque	0.1	*Panderodus gracilis*	**16.1**	2	37.8

* The bulk conodont samples containing multiple conodont taxa have been described using the following method:
Oz: *Ozarkodina* sp. *Ds*: *Drepanoistodus suberectus*
Ph: *Phragmodus* sp. *Ao*: *Amorphognathus ordovicicus*
Pg: *Panderodus gracilis* *Be*: *Bellodina* sp.

**Groups contain samples that were analyzed and corrected to the same Benzoic acid standard average and have the same standard deviation.
Group 1: corrected Benzoic acid average: 25.43‰, standard deviation: 0.18
Group 2: corrected Benzoic acid average: 22.7‰, standard deviation: 0.47
Group 3: corrected Benzoic acid average: 23.5‰, standard deviation: 0.11

*** Uses Longinelli and Nuti (1973) temperature equation: t°C = 111.4 - 4.3($\delta^{18}O_p$ - $\delta^{18}O_w$)
where δ18Op= δ18O of sample
where δ18Ow= δ18O of water, assumed to be -1 VSMOW
where t = estimated temperature (in degrees C) of water during mineral secretion

B. $\delta^{18}O$ Postville Roadcut and Quarry Data Table

sample	formation	meters above base	conodont*/grain type	$\delta^{18}O$ V-SMOW (corrected)	group**	estimated t°C***
P-M Crinoid 1	Maquoketa	6.2	Phosphatized crinoid	**16.7**	1	35.2
P-M Crinoid 1	Maquoketa	6.2	Phosphatized crinoid	**16.8**	1	34.8
P-M Crinoid 2	Maquoketa	6.2	Phosphatized crinoid	**16.8**	1	34.8
P-M Crinoid 2	Maquoketa	6.2	Phosphatized crinoid	**17.8**	1	30.5
P-M Crinoid 3	Maquoketa	6.2	Phosphatized crinoid	**17.7**	1	30.9
P-M Crinoid 3	Maquoketa	6.2	Phosphatized crinoid	**17.8**	1	30.5
P-M PO4 Grain 1	Maquoketa	6.2	Phosphatic pellet	**17.8**	1	30.5
P-M PO4 Grain 1	Maquoketa	6.2	Phosphatic pellet	**18**	1	29.7
P-M PO4 Grain 2	Maquoketa	6.2	Phosphatic pellet	**18.1**	1	29.2
P-M PO4 Grain 2	Maquoketa	6.2	Phosphatic pellet	**18.1**	1	29.2
P-M PO4 Grain 3	Maquoketa	6.2	Phosphatic pellet	**17.7**	1	30.9
P- M1 Brach 1 a	Maquoketa	6.2	*Leptobolus, brachiopod*	**17.7**	1	31.1
P- M1 Brach 1 b	Maquoketa	6.2	*Leptobolus, brachiopod*	**18.0**	1	29.7
P- M1 Brach 2 a	Maquoketa	6.2	*Leptobolus, brachiopod*	**18.4**	1	27.8
P- M1 Brach 2 b	Maquoketa	6.2	*Leptobolus, brachiopod*	**18.3**	1	28.4
P-M Brach 1	Maquoketa	6.2	*Leptobolus, brachiopod*	**18**	1	29.7
P-M Brach 1	Maquoketa	6.2	*Leptobolus, brachiopod*	**17.8**	1	30.5
P-M Brach 2	Maquoketa	6.2	*Leptobolus, brachiopod*	**17.6**	1	31.4
P-M Brach 3	Maquoketa	6.2	*Leptobolus, brachiopod*	**18.5**	1	27.5
P-M Brach 3	Maquoketa	6.2	*Leptobolus, brachiopod*	**18**	1	29.7
P- M1 Ao	Maquoketa	6.2	*Amorphognathus ordovicus*	**19.7**	3	22.4
P- M1 bulk	Maquoketa	6.2	*Ozarkodina, Panderodus gracilis*	**19.9**	3	21.7
P- M1 Ds	Maquoketa	6.2	*Drepanoistodus suberectus*	**18.6**	3	27.3
P- M1 Ao	Maquoketa	6.2	*Amorphognathus ordovicus*	**19.8**	1	21.8
P- M1 Ds	Maquoketa	6.2	*Drepanoistodus suberectus*	**18.7**	1	26.5
P-D1 Ao a	Dubuque	5.8	*Amorphognathus ordovicus*	**18.6**	1	27.1
P-D1 Ao b	Dubuque	5.8	*Amorphognathus ordovicus*	**18.9**	1	25.8
P-D1 Ds a	Dubuque	5.8	*Drepanoistodus suberectus*	**18.0**	1	29.7
P-D1 Ds b	Dubuque	5.8	*Drepanoistodus suberectus*	**17.9**	1	30
P-D1 O c	Dubuque	5.8	*Ozarkodina*	**19.4**	1	23.6

P-D1 O b	Dubuque	5.8	*Ozarkodina*	**19.3**	1	23.9
P-D1 O a	Dubuque	5.8	*Ozarkodina*	**19.3**	1	24.2
P- D2 bulk	Dubuque	5.6	*Pg, Ds*	**19.5**	3	23.4
P- D2 Oz	Dubuque	5.6	*Ozarkodina*	**19.3**	3	24
P-D3 Pb	Dubuque	5	*Panderodus gracilis*	**19.2**	3	24.6
P-D3 Pc	Dubuque	5	*Panderodus gracilis*	**19.0**	3	25.2
P-D3 Pd	Dubuque	5	*Panderodus gracilis*	**19.0**	3	25.3
P-D3 Pe	Dubuque	5	*Panderodus gracilis*	**19.1**	3	25.1
P-D4 Ds	Dubuque	4.6	*Drepanoistodus suberectus*	**18.6**	2	27.1
P-D4 P	Dubuque	4.6	*Panderodus gracilis*	**16.4**	2	36.5
P-D5 Ds	Dubuque	3.9	*Drepanoistodus suberectus*	**18.1**	2	29.2
P-D7 Ds	Dubuque	3.4	*Drepanoistodus suberectus*	**18.3**	2	28.4
P-D7 P	Dubuque	3.4	*Panderodus gracilis*	**16.8**	2	34.8
P- D9 bulk	Dubuque	2.7	*Ds; Pg*	**19.8**	3	22
P- D9 Oz	Dubuque	2.7	*Ozarkodina*	**19.5**	3	23.4
P-D10	Dubuque	2.5	*Ph, Ao, Oz*	**19.4**	3	23.6
P-D11 bulk	Dubuque	1.3	*Oz; Ds; Pg; Ao*	**17.8**	3	30.5
P- D11 bulk 1	Dubuque	1.3	*Oz; Ds; Pg; Ao*	**18.9**	3	25.7
P- D11 Ds	Dubuque	1.3	*Drepanoistodus suberectus*	**18.5**	3	27.6
P- D11 Oz	Dubuque	1.3	*Ozarkodina*	**19.5**	3	23.3

* The bulk conodont samples containing multiple conodont taxa have been described using the following method:
Oz: *Ozarkodina* sp. *Ds*: *Drepanoistodus suberectus*
Ph: *Phragmodus* sp. *Ao*: *Amorphognathus ordovicicus*
Pg: *Panderodus gracilis* *Be*: *Bellodina* sp.

**Groups contain samples that were analyzed and corrected to the same Benzoic acid standard average and have the same standard deviation.
Group 1: corrected Benzoic acid average: 25.43‰, standard deviation: 0.18
Group 2: corrected Benzoic acid average: 22.7‰, standard deviation: 0.47
Group 3: corrected Benzoic acid average: 23.5‰, standard deviation: 0.11

*** Uses Longinelli and Nuti (1973) temperature equation: t°C = 111.4 - 4.3($\delta^{18}O_p$ - $\delta^{18}O_w$)
where δ18Op= δ18O of sample
where δ18Ow= δ18O of water, assumed to be -1 VSMOW
where t = estimated temperature (in degrees C) of water during mineral secretion

C. $\delta^{18}O$ Rifle Hill Roadcut and Quarry Data Table

sample	formation	meters above base	conodont*/grain type	$\delta^{18}O$ V-SMOW (corrected)	group**	estimated t°C***
RH- M7 Oz	Maquoketa	11.5	*Ozarkodina*	**20.9**	3	17.2
RH- M7 DS	Maquoketa	11.5	*Drepanoistodus suberectus*	**19.6**	3	22.8
RH- M4 brach	Maquoketa	8	*Leptobolus,* brachiopod	**19.8**	3	21.9
RH-D1 DS	Dubuque	1	*Drepanoistodus suberectus*	**17.7**	3	30.7
RH- D9 brach 1	Dubuque	5.4	*Leptobolus,* brachiopod	**19.7**	3	22.3
RH- D9 brach 2	Dubuque	5.4	*Leptobolus,* brachiopod	**20.1**	3	20.6
RH- D6 brach	Dubuque	3.9	*Leptobolus,* brachiopod	**19.3**	3	24.1
RH- D3 brach 1	Dubuque	2.4	*Leptobolus,* brachiopod	**19.5**	3	23.2
RH- D3 brach 2	Dubuque	2.4	*Leptobolus,* brachiopod	**19.6**	3	22.8

* The bulk conodont samples containing multiple conodont taxa have been described using the following method:
Oz: *Ozarkodina* sp. *Ds*: *Drepanoistodus suberectus*
Ph: *Phragmodus* sp. *Ao*: *Amorphognathus ordovicicus*
Pg: *Panderodus gracilis* *Be*: *Bellodina* sp.

**Groups contain samples that were analyzed and corrected to the same Benzoic acid standard average and have the same standard deviation.
Group 1: corrected Benzoic acid average: 25.43‰, standard deviation: 0.18
Group 2: corrected Benzoic acid average: 22.7‰, standard deviation: 0.47
Group 3: corrected Benzoic acid average: 23.5‰, standard deviation: 0.11

*** Uses Longinelli and Nuti (1973) temperature equation: $t°C = 111.4 - 4.3(\delta^{18}O_p - \delta^{18}O_w)$
where $\delta 18Op = \delta 18O$ of sample
where $\delta 18Ow = \delta 18O$ of water, assumed to be -1 VSMOW
where t = estimated temperature (in degrees C) of water during mineral secretion

D. Unused $\delta^{18}O$ Data

sample	formation	conodont*/grain type	$\delta^{18}O$ V-SMOW	error	estimated t°C***
P- M1 Ds 2	Maquoketa	*Drepanoistodus suberectus*	**17.8**	phosphate rind on conodont	30.5
P-D2 bulk	Dubuque	*Pg; Ds*	**23.2**	chemistry procedure error	7.3
P-D3 Pa	Dubuque	*Panderodus gracilis*	**18.6**	one of 5 replicates, .4‰ off	27.1
P- D11 bulk 2	Dubuque	*Oz; Ds; Pg; Ao*	**21.2**	highest value, .4‰ off	15.8
RH- M7 Ds	Maquoketa	*Drepanoistodus suberectus*	**16.5**	low yield	36.1
RH- D1 Ds	Dubuque	*Drepanoistodus suberectus*	**16.6**	low yield	35.7
WQ-M10 Oz	Maquoketa	Ozarkodina	**15.1**	low yield	42.1
WQ-M5 Oz	Maquoketa	Ozarkodina	**15.4**	low yield	40.8
WQ-P1 DS a	Phosphate Horizon	Drepanoistodus suberectus	**44.1**	chemistry procedure error	-82.5
WQ-D10 DS	Dubuque	Drepanoistodus suberectus	**67.1**	chemistry procedure error	-181.4
WQ- D6 bulk	Dubuque	*Pg; Ds*	**19.0**	low yield	25.2
WQ- M7 brach	Maquoketa	*Leptobolus, brachiopod*	**17.5**	low yield	31.8
WQ- M9 bulk	Maquoketa	*Ds; Pg*	**21.1**	low yield	16.2
WQ- P1 DS 3	Phosphate Horizon	*Drepanoistodus suberectus*	**19.8**	low yield	21.8
WQ-D3 Ds 1	Dubuque	Drepanoistodus suberectus	**18.3**	low yield	28.4
WQ- D3 Ds 2	Dubuque	Drepanoistodus suberectus	**18.4**	low yield	27.9
WQ- D8 Ds	Dubuque	Drepanoistodus suberectus	**19.5**	low yield	23.2
WQ- M6 brach	Maquoketa	Leptobolus, brachiopod	**17.4**	low yield	32.2
WQ- D5 bulk	Dubuque	Pg; Ds; unidentified fragments	**24.9**	odd value	0

* The bulk conodont samples containing multiple conodont taxa have been described using the following method:
Oz: *Ozarkodina* sp. *Ds*: *Drepanoistodus suberectus*
Ph: *Phragmodus* sp. *Ao*: *Amorphognathus ordovicicus*
Pg: *Panderodus gracilis* *Be*: *Bellodina* sp.

**Groups contain samples that were analyzed and corrected to the same Benzoic acid standard average and have the same standard deviation.
Group 1: corrected Benzoic acid average: 25.43‰, standard deviation: 0.18
Group 2: corrected Benzoic acid average: 22.7‰, standard deviation: 0.47
Group 3: corrected Benzoic acid average: 23.5‰, standard deviation: 0.11

*** Uses Longinelli and Nuti (1973) temperature equation: $t°C = 111.4 - 4.3(\delta^{18}O_p - \delta^{18}O_w)$
where δ18Op= δ18O of sample
where δ18Ow= δ18O of water, assumed to be -1 VSMOW
where t = estimated temperature (in degrees C) of water during mineral secretion

E. $\delta^{18}O$ Standards

Standard	$\delta^{18}O$ V-SMOW (corrected)	group
Benzoic acid	23.1	2
Benzoic acid	23.3	2
Benzoic acid	22.9	2
Benzoic acid	23	2
Benzoic acid	22.8	2
Benzoic acid	22.5	2
Benzoic acid	22.5	2
Benzoic acid	21.5	2
Benzoic acid	22.9	2
Benzoic acid	22.5	2
Benzoic acid	23.4	3
Benzoic acid	23.8	3
Benzoic acid	23.6	3
Benzoic acid	23.4	3
Benzoic acid	23.2	3
Benzoic acid	23.5	3
Benzoic acid	23.5	3
Benzoic acid	23.5	3
Benzoic acid	23.5	3
Benzoic acid	23.5	3
Benzoic acid	23.5	3
Benzoic acid	23.4	3
Benzoic acid	23.6	3
Benzoic	23.6	3

acid		
Benzoic acid	23.5	3
Benzoic acid	23.3	3
Benzoic acid	23.6	3
Benzoic acid	23.4	3
Benzoic acid	23.6	3
Benzoic acid	25.3	1
Benzoic acid	25.2	1
Benzoic acid	25.3	1
Benzoic acid	25.5	1
Benzoic acid	25.3	1
Benzoic acid	25.7	1
Benzoic acid	25.3	1
Benzoic acid	25.2	1
Benzoic acid	25.4	1
Benzoic acid	25.2	1
Benzoic acid	25.5	1
Benzoic acid	25.3	1
ACROS	14.4	3
ACROS	14.3	3
ACROS	14.5	3
ACROS	14.2	3
ACROS	13.7	3
ACROS	14.5	3
ACROS	14.2	3
ACROS	14.0	3
ACROS	14.3	3
ACROS	14.0	3
ACROS	14.1	3
ACROS	13.8	3
ACROS	14.4	3
ACROS	14.0	3
ACROS	13.4	3

ACROS	13.5	3
ACROS	13.6	3
ACROS	13.3	2
ACROS	13.1	2
ACROS	13	2
ACROS	12	2
ACROS	12.7	1
ACROS	12.9	1
ACROS	12.8	1
ACROS	13.4	1
ACROS	11.4	2
ACROS	12.7	2

** Groups contain samples that were analyzed and corrected to the same Benzoic acid standard average and have the same standard deviation.
Group 1: corrected Benzoic acid average: 25.43‰, standard deviation: 0.18
Group 2: corrected Benzoic acid average: 22.7‰, standard deviation: 0.47
Group 3: corrected Benzoic acid average: 23.5‰, standard deviation: 0.11

F. $\varepsilon_{Nd(t)}$ Webber Quarry Data Table

1 sample	2 meters	3 age	4 $^{147}Sm/^{144}Nd$ avg	5 $^{143}Nd/^{144}Nd$ (measured)	6 error	7 $\varepsilon_{Nd(0)}$	8 e^lt	9 e^lt-1	10 correction factor	11 143/144 (initial)	12 measured-initial	13 CHUR	14 $\varepsilon_{Nd(t)}$
WQ-M10	13.3	448.00	0.11727	0.512111	4.00E-06	-10.3	1.002916244	0.002916244	3.41996E-04	0.5117692	0.000342	0.5120644	**-5.76**
WQ-M9	12.6	448.00	0.11727	0.512158	1.30E-05	-9.4	1.002916244	0.002916244	3.41996E-04	0.5118162	0.000342	0.5120644	**-4.85**
WQ-M7	10.2	448.00	0.11727	0.512157	7.20E-06	-9.4	1.002916244	0.002916244	3.41996E-04	0.5118152	0.000342	0.5120644	**-4.87**
WQ-M6	8.3	448.00	0.11727	0.512153	5.70E-06	-9.5	1.002916244	0.002916244	3.41996E-04	0.5118112	0.000342	0.5120644	**-4.94**
WQ-M5	7.9	448.00	0.11727	0.512108	4.20E-06	-10.3	1.002916244	0.002916244	3.41996E-04	0.5117662	0.000342	0.5120644	**-5.82**
WQ-M4	7.4	448.00	0.11727	0.512142	8.40E-06	-9.7	1.002916244	0.002916244	3.41996E-04	0.5118002	0.000342	0.5120644	**-5.16**
WQ-M3	6.9	448.00	0.11727	0.512114	6.00E-06	-10.2	1.002916244	0.002916244	3.41996E-04	0.5117722	0.000342	0.5120644	**-5.71**
WQ-M1	5.8	448.00	0.11727	0.512079	6.30E-06	-10.9	1.002916244	0.002916244	3.41996E-04	0.5117372	0.000342	0.5120644	**-6.39**
WQ-P2	5.25	448.00	0.11727	0.512107	7.40E-06	-10.4	1.002916244	0.002916244	3.41996E-04	0.5117652	0.000342	0.5120644	**-5.84**
WQ-P1	5.07	448.00	0.11727	0.512113	5.10E-06	-10.2	1.002916244	0.002916244	3.41996E-04	0.5117712	0.000342	0.5120644	**-5.73**
WQ-D11	4.95	448.00	0.11727	0.512061	6.20E-06	-11.3	1.002916244	0.002916244	3.41996E-04	0.5117192	0.000342	0.5120644	**-6.74**
WQ-D10	4.6	448.00	0.11727	0.512052	6.30E-06	-11.4	1.002916244	0.002916244	3.41996E-04	0.5117102	0.000342	0.5120644	**-6.92**
WQ-D9	4.1	448.00	0.11727	0.512031	6.70E-06	-11.8	1.002916244	0.002916244	3.41996E-04	0.5116892	0.000342	0.5120644	**-7.33**
WQ-D8	3.6	448.00	0.11727	0.512041	4.40E-06	-11.6	1.002916244	0.002916244	3.41996E-04	0.5116992	0.000342	0.5120644	**-7.13**
WQ-D7	3.1	448.00	0.11727	0.512070	6.00E-06	-11.1	1.002916244	0.002916244	3.41996E-04	0.5117282	0.000342	0.5120644	**-6.57**
WQ-D6	2.6	448.00	0.11727	0.512034	6.10E-06	-11.8	1.002916244	0.002916244	3.41996E-04	0.5116922	0.000342	0.5120644	**-7.27**
WQ-D5	2.1	448.00	0.11727	0.512014	5.10E-06	-12.2	1.002916244	0.002916244	3.41996E-04	0.5116722	0.000342	0.5120644	**-7.66**
WQ-D4	1.4	448.00	0.11727	0.512016	3.80E-06	-12.1	1.002916244	0.002916244	3.41996E-04	0.5116742	0.000342	0.5120644	**-7.62**
WQ-D3	1.2	448.00	0.11727	0.511965	5.90E-06	-13.1	1.002916244	0.002916244	3.41996E-04	0.5116232	0.000342	0.5120644	**-8.62**
WQ-D2	0.6	448.00	0.11727	0.511983	5.60E-06	-12.8	1.002916244	0.002916244	3.41996E-04	0.5116412	0.000342	0.5120644	**-8.26**
WQ-D1	0.1	448.00	0.11727	0.511987	4.00E-06	-12.7	1.002916244	0.002916244	3.41996E-04	0.5116452	0.000342	0.5120644	**-8.19**

1: Sample name
2: Stratigraphic position of samples in meters. WQ-D1 is the oldest sample while WQ-M10 is the youngest.
3: Age in millions of years used for all calcuations.
4: The average $^{147}Sm/^{144}Nd$ of samples calculated from the ^{147} Sm and ^{144}Nd values of samples WQ-D4,D7,D11,P2 and M9.
5: The measured $^{143}Nd/^{144}Nd$ ratio.
6: Reported error.
7: $\varepsilon_{Nd(0)} = ((^{143}Nd/^{144}Nd_{(sample)}/CHUR)-1)*10^4$, where CHUR is the chondritic uniform reservoir =0.512638
8: $= e^{(0.0000065*age)}$
9: $= e^{(0.0000065*age)}-1$
10: correction factor $=(e^{(0.0000065*age)}-1)(^{147}Sm/^{144}Nd$ avg)
11: $^{143}Nd/^{144}Nd_{(initial)} = {}^{147}Sm/^{144}Nd$ avg-$((e^{(0.0000065*age)}-1)(^{147}Sm/^{144}Nd$ avg))
12: $= {}^{143}Nd/^{144}Nd_{(measured)} - {}^{143}Nd/^{144}Nd_{(initial)}$
13: CHUR(chondritic uniform reservoir)= 0.512064
14: $\varepsilon_{Nd(t)}=((^{143}Nd/^{144}Nd_{(initial)}/CHUR)-1)*10^4$, where CHUR=0.512064

G. Complete Sample List

Sample	Formation	Location	meters above base
SW- M1	Maquoketa	South Williams Core	756.7
SW- M2	Maquoketa	South Williams Core	760.9
SW- M3	Maquoketa	South Williams Core	763.4
SW- M4	Maquoketa	South Williams Core	765.5
SW- M5	Maquoketa	South Williams Core	767.9
SW- M6	Maquoketa	South Williams Core	770
SW- D1	Dubuque	South Williams Core	772.1
SW- D2	Dubuque	South Williams Core	775.8
SW- D3	Dubuque	South Williams Core	777.7
SW- D4	Dubuque	South Williams Core	780.7
SW- D5	Dubuque	South Williams Core	782.3
SW- D6	Dubuque	South Williams Core	785.6
BS5- 1	Maquoketa	Big Springs Core	263.7
BS5- 2	Maquoketa	Big Springs Core	277.5
BS5- 3	Maquoketa	Big Springs Core	294
Graf- 1 float	Maquoketa	Graf, IA	N/A
Graf- 1 shale	Maquoketa	Graf, IA	5.6
Graf- 1- 3	Maquoketa	Graf, IA	4.7
Upper Maq 1	Maquoketa	Hwy. 20	4.6
Upper Maq 2	Maquoketa	Hwy. 20	9.4
WQ- M10	Maquoketa	Webber Quarry	13.3
WQ- M9	Maquoketa	Webber Quarry	12.6
WQ- M8	Maquoketa	Webber Quarry	11.2
WQ- M7	Maquoketa	Webber Quarry	10.2
WQ- M6	Maquoketa	Webber Quarry	8.3
WQ- M5	Maquoketa	Webber Quarry	7.9
WQ- M4	Maquoketa	Webber Quarry	7.4
WQ- M3	Maquoketa	Webber Quarry	6.9
WQ- M2	Maquoketa	Webber Quarry	6.4
WQ- M1	Maquoketa	Webber Quarry	5.8
WQ- P2	Phosphate Horizon	Webber Quarry	5.2
WQ- P1	Phosphate Horizon	Webber Quarry	5.1
WQ- D11	Dubuque	Webber Quarry	4.9
WQ- D10	Dubuque	Webber Quarry	4.6
WQ- D9	Dubuque	Webber Quarry	4.1
WQ- D8	Dubuque	Webber Quarry	3.6
WQ- D7	Dubuque	Webber Quarry	3.1
WQ- D6	Dubuque	Webber Quarry	2.6

WQ- D5	Dubuque	Webber Quarry	2.1
WQ- D4	Dubuque	Webber Quarry	1.4
WQ- D3	Dubuque	Webber Quarry	1.2
WQ- D2	Dubuque	Webber Quarry	0.6
WQ- D1	Dubuque	Webber Quarry	0.1
P- M1	Maquoketa	Postville Quarry	6.2
P- D1	Dubuque	Postville Roadcut	5.8
P- D2	Dubuque	Postville Roadcut	5.6
P- D3	Dubuque	Postville Roadcut	5
P- D4	Dubuque	Postville Roadcut	4.6
P- D5	Dubuque	Postville Roadcut	3.9
P- D6	Dubuque	Postville Roadcut	3.6
P- D7	Dubuque	Postville Roadcut	3.4
P- D8	Dubuque	Postville Roadcut	3.1
P- D9	Dubuque	Postville Roadcut	2.7
P- D10	Dubuque	Postville Roadcut	2.5
P- D11	Dubuque	Postville Roadcut	1.3
RH- M7	Maquoketa	Rifle Hill Roadcut/Quarry	11.5
RH- M6	Maquoketa	Rifle Hill Roadcut/Quarry	10.5
RH- M5	Maquoketa	Rifle Hill Roadcut/Quarry	9.5
RH- M4	Maquoketa	Rifle Hill Roadcut/Quarry	8
RH- M3	Maquoketa	Rifle Hill Roadcut/Quarry	7.5
RH- M2	Maquoketa	Rifle Hill Roadcut/Quarry	7
RH- M1	Maquoketa	Rifle Hill Roadcut/Quarry	5.7
RH- D9	Dubuque	Rifle Hill Roadcut/Quarry	5.4
RH- D8	Dubuque	Rifle Hill Roadcut/Quarry	4.8
RH- D7	Dubuque	Rifle Hill Roadcut/Quarry	4.3
RH- D6	Dubuque	Rifle Hill Roadcut/Quarry	3.9
RH- D5	Dubuque	Rifle Hill Roadcut/Quarry	3.8
RH- D4	Dubuque	Rifle Hill Roadcut/Quarry	3.1
RH- D3	Dubuque	Rifle Hill Roadcut/Quarry	2.4

RH- D2	Dubuque	Rifle Hill Roadcut/Quarry	1.8
RH- D1	Dubuque	Rifle Hill Roadcut/Quarry	1

References

Allison, P.A., Wells, M.R. 2006, Circulation in large ancient epicontinental seas: what was different and why? Palaios, 21: 513-515.

Austin, 1987, In *Conodonts: Investigative techniques & applications* (ed.R. L. Austin), pp. 241–255, Elishorwood Chichester.

Bassett, D., MacLeod, K.G., Miller, J., and Ethington, R., 2007, Oxygen isotopic composition of biogenic phosphate and the temperature of Early Ordovician seawater: PALAIOS, v. 22, p. 98–103.

Berner, R.A., 1994, GEOCARB II: a revised model of atmospheric CO2 over Phanerozoic time. American Journal of Science 294, 56–91.

Berner, R.A., Kothavala, Z., 2001, GEOCARB III: a revised model of atmospheric CO2 over Phanerozoic time. American Journal of Science 301, 182–204.

Brand, U., Tazawa, J., Sano, H., Azmy, K., Lee, X., 2009, Is mid-late Paleozoic ocean-water chemistry coupled with epeiric seawater isotope records? Geology, 37: 823-826.

Branson, E.B. and Mehl, M.G., 1933. Conodonts from the Bainbridge Formation (Silurian) of Missouri. *University of Missouri Studies*, 8: 39-52.

Brenchley, P.J., Marshall, J.D., Carden, J.A.F., Robertson, D.B.R., Long, D.G.F., Meidla, T., Hints, L., and Anderson, T.F., 1994, Bathymetric and isotopic evidence for a short-lived late Ordovician glaciation in a greenhouse period: Geology, v. 22, p. 295–298.

Brenchley, P.J., Carden, G.A., Hints, L., Kaljo, D., Marshall, J.D., Martma, T., Meidla, T., Nolvak, J., 2003. High-resolution stable isotope stratigraphy of Upper Ordovician sequences: constraints on the timing of bioevents and environmental changes associated with mass extinction and glaciation. Geological Society of America Bulletin 115, 89–104.

Fanton K.C. and C. Holmden, 2007, Sea level forcing of carbon isotope excursions in epeiric seas: implications for carbon isotope chemostratigraphy: Canadian Journal of Earth Science, v. 44, p. 807-818.

James, J.F., 1890, On the Maquoketa shales and their correlation with the

Cincinnati Group of south-western Ohio: American Geologist, v. 5, p. 335-356.

Herrmann A. D., MacLeod, K.G., Leslie, S.A., 2010, Did a volcanic mega-eruption cause global cooling during the Late Ordovician? PALAIOS, 25: *in press*.

Holmden, C., R.A. Creaser, K. Muehlenbachs, S. Leslie, and S.M. Bergstrom, 1998, Isotopic evidence for geochemical decoupling between ancient epeiric seas and bordering oceans: implications for secular curves: Geology, v. 26, p. 567-570.

Holmden C., Creaser R. A., Muehlenbachs, K., Bergstrom S. M., and Leslie, S. A., 1996, Isotopic and elemental systematics of Sr and Nd in 454 Ma biogenic apatites: Implications for paleoseawater studies. *Earth Planet. Sci. Lett.* 142: 425–437.

Joachimski, M.M., Buggisch, W. 2002, Conodont apatite $\delta^{18}O$ signatures indicate climatic cooling as a trigger of the Late Devonian mass extinction. Geology, 30: 711-714.

Keto L. S. and Jacobsen S. B., 1987, Nd and Sr isotopic variations of Early Paleozoic oceans. *Earth Planet. Sci. Lett.* 84: 27–41.

Keto L. S. and Jacobsen S. B., 1988, Nd isotopic variations of Phanerozoic paleoceans. Earth Planet. Sci. Lett. 90: 395–410.

Kolata, D.R., Huff, W.D., and Bergstrom, S.M. 2001, The Ordovician Sebree Trough: an oceanic passage to the Midcontinent United States. Geological Society of America Bulletin, 113: 1067-1078.

Kolodny Y., Luz B., and Navon S., 1983, Oxygen isotope variations in phosphates of biogenic apatites, I. Fish bone apatite—rechecking the rules of the game. *Earth Planet. Sci. Lett.* 64: 389–404.

Konigshof, P., 2003. Conodont deformation patterns and textural alteration in Paleozoic conodonts: examples from Germany and France. *Senckenbergiana Lethaea* 83: 149-156.

Ladd, H.S., 1929. The stratigraphy and paleontology of the Maquoketa Shale of Iowa: Iowa Geological Survey Annual Report, v. 34, p. 307–448.

LaPorte, D.F., Holmden, C., Patterson, W.P., Prokopiuk, T. and Eglington, B.M., 2009, Oxygen isotope analysis of phosphate: improved precision using TC/EA CF-IRMS. *J. Mass. Spectrom.,* 44: 879-890.

Ludvigson, G.A., Witzke, B.J., González, L.A., Carpenter, S.J., Schneider, C.L.,

and Hasiuk, F., 2004, Late Ordovician (Turinian– Chatfieldian) carbon isotope excursions and their stratigraphic and paleoceanographic significance. Palaeogeography, Palaeoclimatology, Palaeoecology, 210: 187–214.

Longinelli A. and Nuti S., 1973, Revised phosphate-water isotopic temperature scale. *Earth Planet. Sci. Lett.* 19: 373–376.

O'Neil J. R., Roe J. L., Reinhard E., and Blake R. E., 1994, A rapid and precise method of oxygen isotope analysis of biogenic phosphate. *Isr. J. Earth Sci.* 43: 203–212.

Panchuk, K. M., C. Holmden, and S.A. Leslie, 2006, Local controls on carbon cycling in the Ordovician Midcontinent region of North America with implications for carbon isotope secular curves: Journal of Sedimentary Research, v. 76, p. 200-211.

Patzkowsky, M.E., Slupik, L.M., Arthur, M.A., Pancost, R.D., and Freeman, K.H. 1997. Late Middle Ordovician environmental change and extinction, harbinger of the Late Ordovician or continuation of Cambrian patterns. Geology, 25: 911–914.

Pope, M.C., Steffen, J.B., 2003, Widespread, prolonged late Middle to Late

Ordovician upwelling in North America: a proxy record of glaciation? Geology 31: 63–66.

Putman, K. E., Emerson, N.R., Lehrmann, D., 2008, Micro-invertebrate and conodont paleoecology of the Depauperate Zone in the Upper Ordovician Maquoketa Formation of Luana and Postville Quarries, Northeast Iowa. Geological Society of America *Abstracts with Programs*, 40: 75.

Raatz, W.D., and Ludvigson, G.A. 1996, Depositional environments and sequence stratigraphy of Upper Ordovician epicontinental deep water deposits, eastern Iowa and Minnesota. *In* Paleozoic sequence stratigraphy: views from the North American craton. *Edited by* B.J. Wizke, G.A. Ludvigson, and J. Day. The Geological Society of America, Special Paper 306, pp. 143-159.

Saltzman, M.R., and Young, S.A. 2005. Long-lived glaciation in the Late Ordovician? Isotopic and sequence-stratigraphic evidence from western Laurentia. Geology, 33: 109–112.

Scotese, C.R., and McKerrow, W.S., 1990, Revised world maps and introduction, *in* McKerrow, W.S., and Scotese, C.R., eds., Paleozoic paleogeography and biogeography: Geological Society [London] Memoir 12, p. 1–21.

Scotese, C.R., 1997. Paleogeographic Atlas. University of Texas, Arlington, USA.

Simo, J.A., Emerson, N.R., Byers, C.W., and Ludvigson, G.A. 2003. Anatomy of an embayment in an Ordovician epeiric sea, Upper Mississippi Valley, USA. Geology, 31: 545–548.

Trotter, J.A., Williams, I.S., Barnes, C.R., Lécuyer, C., and Nicoll, R.S., 2008, Did cooling oceans trigger Ordovician biodiversication?: Evidence from conodont thermometry: Science, v. 321, p. 550–554.

Vennemann, T.W., Fricke, H.C., Blake, R.E., O'Neil, J.R., Colman, A. 2002, Oxygen isotope analysis of phosphate: a comparison of techniques for analysis of Ag_3PO_4. Chemical Geology, 185: 321-336.

Wenzel, B., LeCuyer, C., and Joachimski, M.M., 2000, Comparing oxygen isotope records of Silurian calcite and phosphate; ^{18}O compositions of brachiopods and conodonts: Geochimica et Cosmochimica Acta, v. 64, p. 1859–1872.

Witzke, B.J., 1980, Middle and Upper Ordovician paleogeography of the region bordering the Transcontinental Arch, *in* Fouch, T.D., and Magathan, E.R., eds., Paleozoic paleogeography of the west-central United States: Rocky Mountain Section, Society of Economic Paleontologists and Mineralogists, p. 1–18.

Witzke, B.J. 1987, Models for circulation patterns in epicontinental seas applied to Paleozoic facies of North America Craton: Paleoceanography, v. 2/2, p. 229-248.

Witzke, B.J., Heathcote, R.C., and Anderson, R.R., 1997, Ordovician Galena Group strata in the Dubuque area, in Witzke, B.J., Bettis, E.A., Anderson, R.R., and Heathcote, R.J., Geology in the Dubuque area: Geol. Soc. Iowa, Guidebook 63, p.7-12.

Witzke, B.J., and Kolata, D.R., 1988, Changing structural and depositional patterns, Ordovician Champlainian and Cincinnatian series of Iowa-Illinois, in Ludvigson, G.A., and Bunker, B.J., eds., New perspectives on the Paleozoic history of the Upper Mississippi Valley: Iowa Geol. Survey, Guidebook no. 8, p. 55-77.